

1 Reviewing the puzzling intracontinental termination of the
2 Araçuaí-West Congo orogenic belt and its implications for
3 orogenic development

4 Carolina Cavalcante ^{a*}, Haakon Fossen^b, Renato Paes de Almeida^c, Maria
5 Helena B.M. Hollanda^c, Marcos Egydio-Silva^c

6 ^a*Departamento de Geologia, Universidade Federal do Paraná, Avenida Coronel Francisco H dos*
7 *Santos, 100, 81531-980, Curitiba, Paraná, Brazil.*

8 ^b*Museum of Natural History/ Department of Earth Science, University of Bergen, Allégaten 41, N-*
9 *5007 Bergen, Norway.*

10 ^c*Instituto de Geociências, Universidade de São Paulo, Rua do Lago, 562, Cidade Universitária, São*
11 *Paulo-SP CEP 05508-900, Brazil.*

12
13
14 **Abstract**

15 Palinspastic reconstructions suggest that the late Proterozoic–Cambrian Brasileiro/Pan-
16 African orogenic belt in southeast Brazil and west Congo terminated northwards into an
17 embayment within the São Francisco-Congo cratonic unit. The orogenic shortening that
18 created the Araçuaí-West Congo orogen in this embayment has been explained by
19 tightening of the horseshoe-shaped São Francisco-Congo craton in a fashion referred to as
20 “nutcracker tectonics”. We show that this model is incompatible with the general orogenic
21 evolution proposed in recent literature, which involves (1) ~50 m.y. of subduction of
22 oceanic crust and associated arc formation, followed by (2) collisional orogeny and crustal
23 thickening. Quantitative considerations show that the original nutcracker model is too rigid

*Corresponding author (geanecarol@gmail.com)

24 to explain even the second, crustal thickening part, let alone any long pre-collisional
25 history. To soften the model, we suggest that the so-called São Francisco – Congo bridge
26 was broken by a ~150 km wide orogenic corridor along the current African Atlantic
27 margin. This corridor adds sufficient mobility to the system to explain the orogenic
28 thickening of the crust to 60-65 km. However, even with this additional softening the
29 confined nature of this orogen is incompatible with prolonged arc development. We
30 therefore suggest that oceanic crust was nonexistent or very limited in the Macaúbas basin,
31 and reject the widely published model involving ~50 m.y. of subduction of oceanic crust
32 and related arc development. Instead, we find strong support for a hot intracontinental
33 orogen model in the currently available P-T, geochronologic, petrographic and structural
34 data. In this model, extensive melting and flow of the middle crust is likely to have caused
35 spreading of the upper crust in an orogenic setting that was created by collisions along the
36 N, W and S margins of the São Francisco craton from ~630 Ma.

37 *Keywords:* Hot orogen; Confined orogen; Partial melting; Brasiliano/Pan-African belt

38

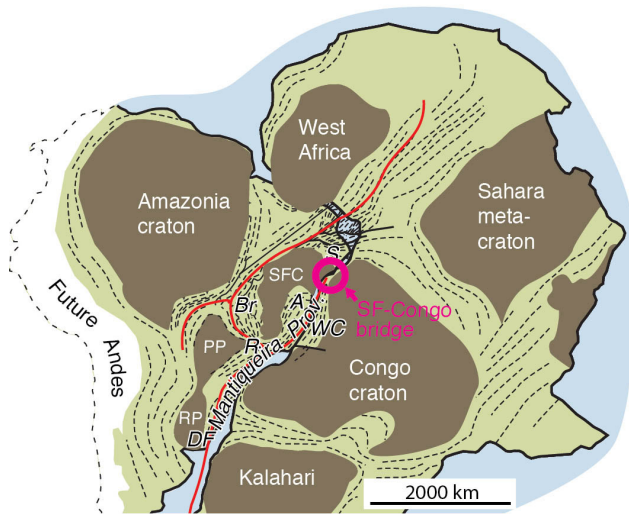
39 **1. Introduction**

40 Mountain belts tend to form connected systems that cross entire continents or
41 supercontinents, such as the extensive Alpine-Himalayan orogenic system running from
42 Asia through the Mediterranean region, the Paleozoic Caledonide-Appalachian system and
43 the mostly Neoproterozoic Brasiliano-Pan-African system. Within these systems,
44 individual orogenic elements form a connected network in which they change character
45 between orthogonal, oblique and strike-slip, but rarely terminate without transfer of

46 displacement to other plate-tectonic elements. And where they do, they tend to do so
47 gradually.

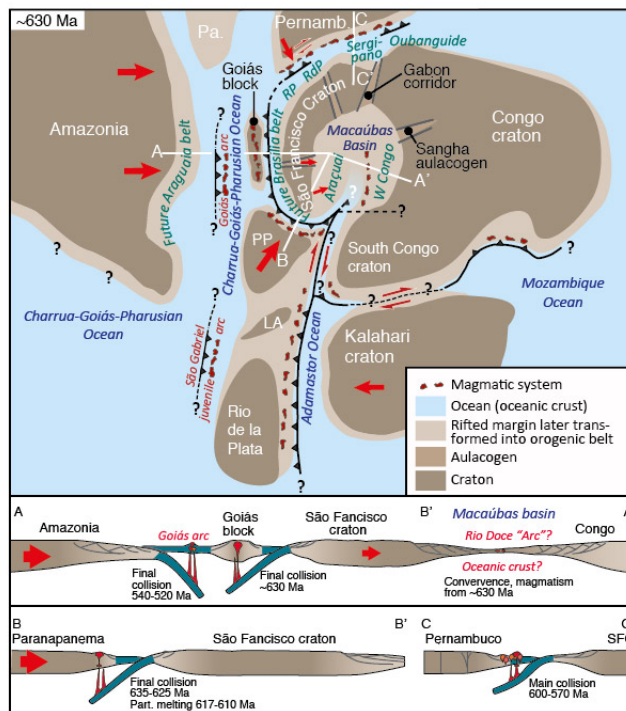
48 The Araçuaí-West Congo orogenic belt developed by shortening of a pre-orogenic rift
49 basin with or without oceanic crust (see discussion below), and the orogen is generally
50 regarded to terminate abruptly into a rigid cratonic continental environment largely
51 unaffected by the Brasiliano/Pan-African deformation (Figs. 1 and 2). The kinematics of
52 the orogen is orthogonal shortening, mostly E-W but radial in the northern part. As
53 discussed below, the Brasiliano/Pan-African Araçuaí-West Congo belt involves substantial
54 crustal thickening and horizontal shortening even close to its northern termination, and thus
55 appears to represent a rather odd example of an orogen that abruptly vanishes into a
56 continental cratonic environment. More specifically, it is surrounded by Archean and
57 Paleoproterozoic continents to the east (Congo craton), north and west (São Francisco
58 craton), and throughout its late Proterozoic orogenic evolution the Araçuaí-West Congo
59 orogenic belt has therefore been classified as a confined (Pedrosa-Soares et al., 2001) or
60 partially confined (Alkmim et al., 2006) orogen.

61



62

63 **Figure 1.** Brasiliano-Pan-African orogenic belts of West Gondwana prior to the formation
 64 of the South Atlantic ocean. A= Araçuaí; Br=Brasília orogen; DF=Dom Feliciano belt;
 65 PP= Paranapanema Craton; RP=Rio de La Plata craton; SFC=São Francisco craton;
 66 WC=West Congo.



67

68 **Figure 2.** Schematic tectonic setting immediately prior to the main collisional events
 69 between the São Francisco craton and surrounding cratonic and magmatic elements.

70 *Cross-sections through different parts of the margin are shown. Note that most authors*
71 *since the late 1990s consider the Macaúbas Basin, which develops into the Araçuaí-W*
72 *Congo orogen, to have hosted an ocean that started to subduct at this time (630 Ma) and*
73 *until ~580 Ma (e.g., Pedrosa-Soares et al., 1998). LA=Luis Alves, PP=Paranapanema,*
74 *RP= Rio Preto belt; RdP=Riacho do Pontal belt. Based in part on Meira et al. (2016).*
75

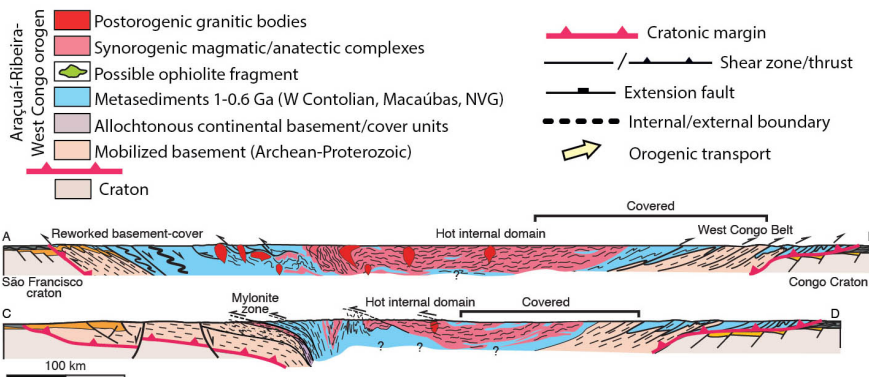
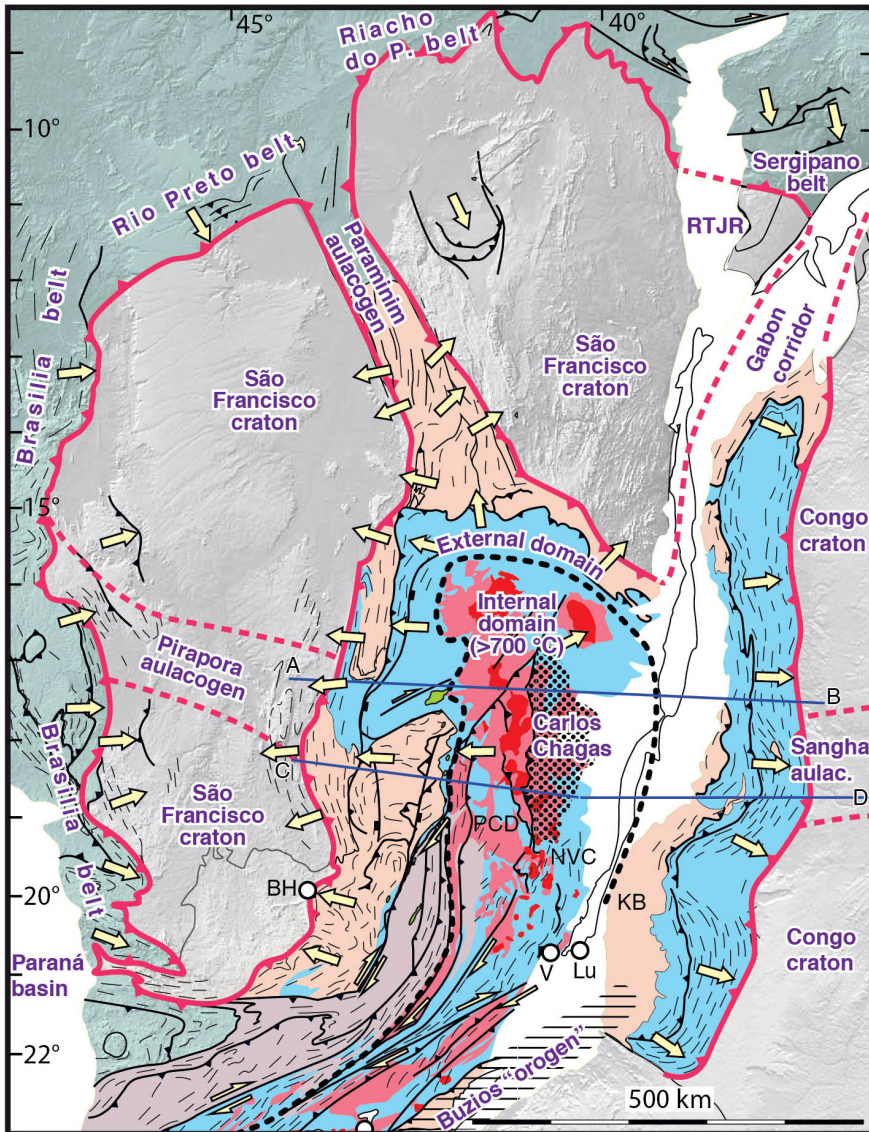
76 The concept of a confined or “dead end” orogen is special, and its boundary
77 conditions impose important constraints on the kinematic, strain and tectonic evolution of
78 such orogenic systems. These conditions have not been sufficiently taken into consideration
79 in the case of the Araçuaí-West Congo orogenic belt, and we here critically discuss the so-
80 called confined model in the light of these boundary conditions. We conclude that both the
81 existing confined orogenic model (“nutcracker tectonics”; Alkmim et al., 2006) and the
82 widely published tectonic model for the orogenic evolution (e.g., Pedrosa-Soares et al.,
83 1998; 2001; Gradim et al, 2014; Peixoto et al., 2015; Gonçalves et al., 2016; Richter et al.,
84 2016; Tedeschi et al., 2016; Alkmim et al., 2017; Degler et al., 2017) need fundamental
85 modifications, and argue that the orogenic evolution is better understood in terms of a hot
86 orogen model (Vanderhaeghe, 2009; Jamieson and Beaumont, 2013) without prolonged
87 oceanic subduction and magmatic arc development. We also point at data needed to better
88 understand the evolution of this intriguing branch of the Brasiliano/Pan-African orogenic
89 system.

90

91 **2. General setting of the orogenic system**

92 Reconstruction of the West Gondwana paleocontinent (Fig. 1) shows the Araçuaí-West
93 Congo orogenic belt as a part of the Neoproterozoic Brasiliano/Pan-African orogenic

94 system (Torsvik and Cocks, 2013). This orogenic system is defined by a network of
95 orogenic belts formed by amalgamation of a plethora of larger and smaller cratonic
96 continents into West Gondwana in the Neoproterozoic-Cambrian, following extensive
97 Neoproterozoic rifting (Trompette, 1994, 2000). The Araçuaí-West Congo orogen is the
98 northern part of one of these belts, known as the Mantiqueira province. This province
99 stretches from Uruguay and northwards along the southeast coast of Brazil, and formed
100 during convergent movements between the São Francisco, Congo, Kalahari, Rio de la Plata,
101 and Paranapanema cratons (Fig. 1). The Ribeira belt is the central section of the
102 Mantiqueira province, and connects the Dom Feliciano and Araçuaí-West Congo belt belts
103 (Fig. 1). The restored width of the Araçuaí-West Congo orogenic belt is ~650-700 km,
104 about twice that of the transpressional Ribeira belt to the south (Fig. 3). In the following we
105 will describe the São Francisco-Congo craton and the Araçuaí-West Congo and associated
106 orogenic belts, before discussing the problems associated with the current model and
107 suggesting an alternative evolutionary model for the Araçuaí-West Congo orogen.
108



109

110 **Figure 3.** Simplified geologic map of the Araçuaí-West Congo and northern Ribeira
 111 orogen, with Congo restored to its pre-Atlantic rifting situation with respect to South

112 *America. Yellow arrows represent kinematics during the main/late stages of orogeny, and*
113 *are in part from Alkmim et al. (2006). Based on maps from the Geological Survey of Brazil*
114 *(CPRM) and Tack et al. (2001). Cross-sections are based on Tack et al. (2001), Alkmim et*
115 *al. (2006), and Vauchez et al. (2007). Metasediments 1-0.6 Ga (blue) range from very low*
116 *grade in the foreland to high-T paragneisses in the hot internal zone of the orogen. Dotted*
117 *ornament indicate the Carlos Chagas anatectic domain. BH=Belo Horizonte;*
118 *KB=Kimezian basement (reworked); Lu=Luanda; NVC=Nova Venécia Complex;*
119 *PCD=Plutonic Central Domain of Mondou (2012); RJ=Rio de Janeiro; RTJR=Recôncavo-*
120 *Tucano-Jatoba rift; SP=Sao Paulo; V=Vitoria. Geographic coordinates refer to current*
121 *Brazil.*

122

123

124 *2.1 The São Francisco-Congo craton and its rift arms*

125 The São Francisco-Congo craton consists of Archean and Paleoproterozoic rock
126 complexes older than ~1.8 Ga, covered by a variety of supracrustal rocks of late
127 Paleoproterozoic to late Mesoproterozoic age (Espinhaço Supergroup), followed by the rift
128 and continental margin deposits of the Neoproterozoic Macaúbas Group (Alkmim et al.,
129 2017). Deposition of the Macaúbas Group was related to rifting following the formation of
130 Rhodinia at ~1.0 Ga. Most likely the São Francisco-Congo craton was not part of Rhodinia
131 (Evans et al., 2009; 2016), but this uncertainty does not affect the late Neoproterozoic
132 orogenic development discussed here.

133 The shape of the craton in the study area mimics that of a southward-opening
134 horseshoe (Fig. 2). This shape is broken by several rift arms that were variously reactivated
135 during the Araçuaí-West Congo orogeny. The Paramirim (Cruz and Alkmim, 2017) and
136 Pirapora aulacogens dissect the craton into a southern, northern and northeastern part, and

137 third rift arm, the Sangha aulacogen (Alvarez, 1995), extends into the Congo craton (Fig.
138 3). In addition, a 150-200 km wide north-trending orogenic corridor, informally named the
139 Gabon corridor (Fossen et al., 2017), occurs along the African side of the South Atlantic
140 margin, where the orogenic front continues for several hundred kilometers beyond the
141 termination on the Brazilian side before getting buried under younger deposits (NE part of
142 the map in Fig. 3). The Gabon corridor, which has received little attention in the previous
143 literature, may well be a pre-orogenic rift segment similar to the better-exposed Paramirim
144 aulacogen to the west, but subjected to more intense Pan-African reactivation. If so, it is an
145 important tectonic element that breaks the São Francisco-Congo “bridge” and provided
146 increased flexibility during Neoproterozoic rifting and the Brasiliano orogeny.

147 All of these rift arms radiate from a center located in the northern Araçuaí-West
148 Congo orogen, hinting that a plume may have been located in this location during rifting.
149 The largest rift was trending southwards from this rift center along what is now the
150 Araçuaí-West Congo orogen. As a whole, this rift system accommodated the opening of the
151 pre-orogenic Macaúbas basin in the cratonic embayment, as well as the orogenic shortening
152 across the Araçuaí-West Congo orogen.

153

154 *2.2 The São Francisco-Congo cratonic bridge*

155 A key point in the following discussion is the widely accepted idea that the Congo
156 and São Francisco cratons were physically connected from the Paleoproterozoic until the
157 Cretaceous opening of the Atlantic ocean by what has been referred to as the São
158 Francisco-Congo cratonic bridge (Porada, 1989; Pedrosa-Soares et al., 2001; Alkmim et al.,
159 2006; Barbosa and Barbosa, 2017; Degler et al., 2018). This “cratonic bridge” has been

160 discussed in detail by Alkmim et al. (2006), who presented the following main arguments
161 in favor of a connection between the São Francisco and Congo cratons: 1) lack of
162 Neoproterozoic orogenic deformation along the coast of Bahia and Gabon (a point
163 discussed in Section 5), 2) paleomagnetic poles roughly coinciding for the two sides of the
164 bridge (McWilliams, 1981; D'Agrella Filho et al., 1990, 2004; Renne et al., 1990), and 3)
165 the width of the Atlantic margin being narrow, which they consider to be characteristic of
166 rifted cratonic crust. This cratonic bridge represents a key element in a poorly understood
167 geometric situation that puts important restrictions on the kinematic evolution of the
168 northern part of the Araçuaí-Ribeira-West Congo orogenic system.

169 In spite of the general acceptance of the cratonic bridge, the prevailing tectonic model
170 for the confined orogen south of the cratonic bridge is that of eastward subduction of
171 oceanic crust under the West Congo rifted margin (Fig. 2), and subsequent collision
172 between the West Congo margin and the eastern margin of the São Francisco craton
173 (Pedrosa-Soares et al., 1998; Alkmim et al., 2006; Vauchez et al., 2007). Trompette (1994,
174 1997), on the other hand, considered the Araçuaí-West Congo belt as “partly or totally
175 intracratonic” (Trompette, 2000), with the Adamastor ocean “ending northwards in a
176 complex and wide continental rift system identified in the Araçuaí-Ribeira-West Congo
177 belt” (Trompette, 1994), largely similar to our interpretation shown in Fig. 2.

178

179 *2.3 Brasiliano orogenesis*

180 A protracted Neoproterozoic orogenic history created the Brasiliano orogenic system,
181 which around the São Francisco craton includes the Araçuaí-West Congo-Ribeira orogenic
182 belt along its eastern margin, the Brasilia belt along its southern and western margins, and

183 the Rio Preto, Riacho do Pontal and Sergipano belts to the north (Fig. 2). All of these
184 orogenic belts are connected as parts of the Brasiliano orogenic system, which developed as
185 a result of convergent to oblique interaction between different cratonic and arc elements, in
186 the Brasilia belt from as early as ~900 Ma (Pimentel, 2016). These interactions culminated
187 around 630-600 Ma to form West Gondwana, although orogenic pulses and events locally
188 occurred as late as the early Cambrian (Schmitt, 2004). The São Francisco craton was
189 affected by all of the major collisions, and each of its surrounding belts is briefly
190 summarized in the following.

191

192 *2.3.1 The northern Brasilia belt*

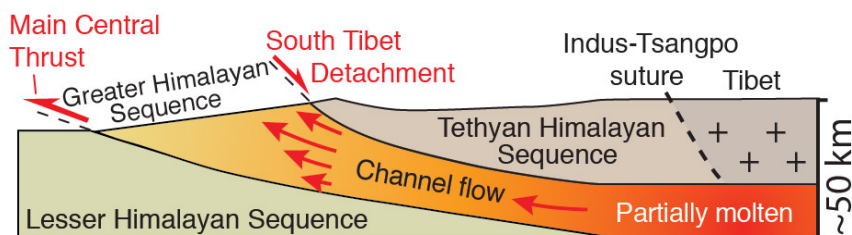
193 The northern Brasilia orogenic belt is the result of collision of the Archean-
194 Proterozoic Goiás microcontinent, the 670-639 Ma Goiás arc, and possibly other magmatic
195 arc systems with the western passive margin of the São Francisco craton. The major
196 continental collisional stage of this convergent history occurred at ~630 Ma (Pimentel,
197 2016; Fuck et al., 2017) or 640-610 Ma (Valeriano et al., 2008). The Amazon craton itself,
198 also moving eastward relative to the São Francisco continent, collided later, probably
199 between 540-520 Ma (Valeriano et al., 2008) or around 550 Ma (Moura et al., 2008) to
200 form the Araguaia belt (Fig. 2). This late concluding event may explain thin-skinned
201 thrusting of the Bambuí Group cover of the São Francisco craton (Reis and Alkmim, 2017).
202 The Bambuí Group has recently been suggested to be as young as 550-542 Ma (Warren et
203 al., 2014). If correct, the Brasilia orogeny seems to have lasted until the dawn of the
204 Cambrian.

205

206 2.3.2 The southern Brasilia belt

207 The southern Brasilia belt was formed by the northward motion of the
208 Paranapanema/Rio de Plata continent, causing accretion of a significant orogenic wedge of
209 allochthonous units onto the southern São Francisco margin. In general, outboard (arc-
210 related) terranes tectonically overlie high-grade units with anatectic domains and
211 retrogressed eclogite, again overlying low-grade units of reworked São Francisco margin
212 affinity (Campos Neto et al., 2011; Valeriano et al., 2008). This pile of thrust nappes
213 developed diachronously with the age of deformation younging toward the São Francisco
214 craton (Campos Neto et al., 2011). Anatectic melting is dated at 617-610 Ma (Martins et
215 al., 2009), and has tentatively been associated with channel flow of the middle crust after
216 crustal thickening (Fig. 4) (Campos Neto et al., 2011). Given the fact that extensive partial
217 melting requires something like 20 Ma of continent-continent collision (Jamieson et al.,
218 2011; Vanderhaeghe, 2009), the main collisional event must have initiated around or before
219 637 Ma, which corresponds well with the 650-630 Ma age suggested by Valeriano (2017).
220 Hence, the main collisional event of the southern Brasilia belt appears to be broadly
221 synchronous with the main event in the northern Brasilia belt.

222



223

224 **Figure 4.** The concept of channel flow (e.g., Nelson et al., 1996) in the context of the
225 Himalayan orogen. Hot and partially molten rocks flow within a channel from the lower or

226 *middle crust toward the foreland under the weight of an overlying orogenic edifice*
227 *(plateau). Modified from Webb et al (2011). Our suggestion is that the hot internal part of*
228 *the Araçuaí-West Congo belt represents an erosional section through the partially molten*
229 *crust.*

230

231 *2.3.3 The Sergipano belt*

232 The Sergipano belt (Fig. 2) is the south-verging orogenic belt located immediately
233 north-northeast of the São Francisco craton. It consists largely of low-grade shelf sediments
234 thrust southward onto the São Francisco craton and intruded by granitic magma. This
235 occurred in response to southward movement of the Pernambuco block to the north from
236 ca. 630 Ma (Oliveira et al., 2006), i.e. contemporaneous with major orogenic activity in the
237 southern and western Brasília belts. Convergent movements appear to have continued at
238 least until 570 Ma, with muscovite defining the pervasive D2 foliation dated at 591±4 Ma
239 (40Ar/39Ar) (Oliveira et al, 2010). Araujo et al. (2013) suggest that this collision happened
240 around 590-580 Ma, contemporaneous with extensive transcurrent shearing in the
241 Pernambuco block (Archanjo et al., 2013). On a larger scale, it connects with the
242 Oubanguide orogen in NW Africa (Trompette, 2000) and the Riacho do Pontal and Rio
243 Preto belt to the west (Fig. 2).

244

245 *2.3.4 The Rio Preto and Riacho do Pontal belts*

246 This 600 km long part of the Brasiliano system borders the São Francisco craton to
247 the north and northwest, and connects with the North Brasília and Sergipano belts (Fig. 2).
248 The Rio Preto and Riacho do Pontal orogenesis involved a pre-Brasiliano (~900 Ma and
249 younger) rift system and passive margin, through a combination of N-S shortening and

250 lateral escape (i.e., partitioned transpression). Collision tectonics is believed to have
251 initiated at around 620 Ma, after a period of northward subduction of oceanic crust and
252 related arc development (Caxito et al., 2017).

253

254 *2.3.5 Timing of collisions around the São Francisco craton*

255 The São Francisco craton was affected by collisions from all of the aforementioned
256 orogenic belts, notably the prolonged collisional history to the west (the northern Brasília
257 orogeny) and collisions in response to north or northeastward motion of the Paranapanema
258 craton to the south. Most of these belts appear to record main collisional events at roughly
259 630 Ma, which seem to have started the shortening of the confined Macaúbas basin and the
260 crustal thickening that lead to the formation of the Araçuaí-West Congo orogen described
261 below. In particular, the prolonged collisional history to the west (the northern Brasília
262 orogeny) and collisions in response to north or northeastward motion of the Paranapanema
263 craton to the south were important for the development of the Araçuaí-West Congo orogen.

264

265 **3. The Araçuaí-West Congo orogen**

266 The Araçuaí-West Congo orogen consists of an external fold-and-thrust belt and a
267 wide and hot internal domain characterized by high temperatures and extensive partial
268 melting and magmatism (Pedrosa-Soares et al., 2001; Vauchez et al., 2007; Cavalcante et
269 al., 2013, 2014, 2016; Alkmim et al., 2017) (Fig. 3). These two parts are separated by a 5
270 km thick high-T/low-P mylonitic thrust zone with top-to-foreland sense of shear, according
271 to Vauchez et al. (2007). The pre-orogenic basin, here referred to as the Macaúbas basin,
272 consists mainly of the up to 10 km thick Macaúbas Group in Brazil and much (~4 km) of

273 the West Congolian Group in Congo, and records mostly the pre-orogenic rift basin history.
274 Initial rifting is constrained by dating of magmatic activity and detrital zircons to around
275 850 Ma in the Macaúbas Group on the São Francisco craton (Alkmim and Martins-Neto,
276 2012 and references therein) with evidence of somewhat earlier rift initiation elsewhere in
277 the Araçuaí-West Congo orogen (Tack et al., 2001; Pedrosa-Soares et al., 2008), and both
278 groups include poorly constrained glacial deposits. Formation of oceanic crust in this basin
279 has been suggested, based on limited occurrences of rather poorly dated (816 ± 72 Ma, Sm-
280 Nd whole-rock isochron) amphibolite and ultramafic rocks on the Brazilian side of the
281 orogen (Pedrosa-Soares et al., 1998).

282 Metasediments and metavolcanics also occur as migmatites and migmatitic granulites
283 in the central part of the orogen. Some of these are probably highly altered sediments of the
284 Macaúbas Group, while other parts (Nova Venécia Complex) have been interpreted as syn-
285 orogenic (back-arc) deposits whose depositional age is bracketed by their youngest detrital
286 zircon age of 606 ± 3 Ma and intrusions dated at 593 ± 8 Ma (Richter et al., 2016).

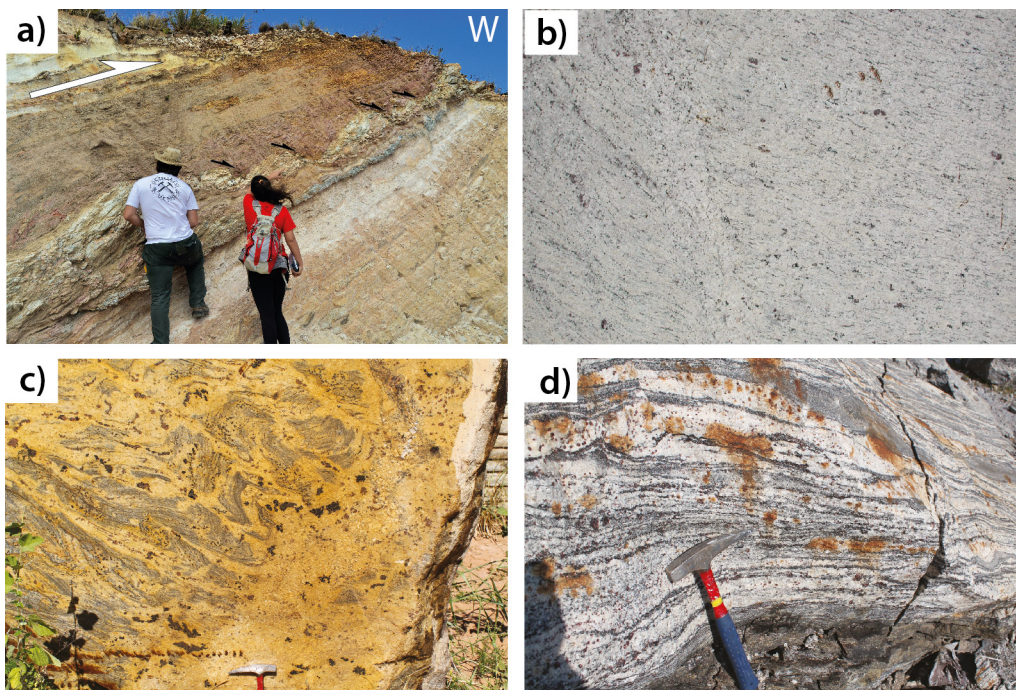
287

288 *3.1 The external fold-and-thrust belt*

289 The external belt of the orogen has a narrow unmetamorphosed to low-grade thin-
290 skinned foreland part that involves the sedimentary succession covering the São Francisco
291 and West Congo continents (Bambuú and West Congolian groups; Tack et al., 2001; Reis
292 and Alkmim, 2015). However, basement involvement is seen relatively close to the
293 orogenic front, locally triggered by reactivation of pre-orogenic rift faults (Alkmim et al.,
294 2017). The metamorphic grade increases into the orogenic belt, where allochthonous
295 basement soon exhibits ductile fabrics of greenschist to amphibolite facies. Mylonitic

296 basement rocks of high-temperature (~750 °C; Vauchez et al., 2007) amphibolite facies
297 occur in the mylonite zone that marks the base of the external domain, with kinematic
298 indicators consistent with thrusting toward the west foreland (e.g., Vauchez et al., 2007). In
299 the southern Araçuaí and into the Ribeira belt, there are also large elongated units of
300 variously sheared magmatic and gneissic rocks interpreted as terranes of both continental
301 margin and arc affinity (Heilbron et al., 2008).

302 The kinematics of this entire external belt is everywhere top-to-the-craton (Figs. 3
303 and 5a), with some local evidence of late extensional reactivation (Marshak et al., 2006).
304 The metamorphic conditions increase progressively from very-low grade along the cratonic
305 margin to amphibolite and granulite facies close to the border of the internal domain
306 (Pedrosa-Soares et al., 2001).



307
308 **Figure 5.** Field aspects of the Araçuaí belt. (a) Asymmetric boudinage in low-grade
309 metasediments showing top-to-foreland (W) thrusting near the thrust front; (b) diatexite

310 *with magmatic foliation marked by aligned biotite and feldspar; c) and d) metatexites*
311 *exhibiting a migmatitic foliation associated with leucosome rich in garnet, forming*
312 *networks of interconnected melt, which suggest high volume (>40%) of magma during*
313 *deformation (i.e., magmatic state deformation).*

314

315 *3.2 The internal domain (hinterland)*

316 The internal hinterland of the Araçuaí-West Congo orogen defines the up to 250 km wide
317 high-temperature core of the orogen, and is made up of high-grade metamorphic rocks and
318 vast amounts of granites and migmatitic rocks that range in crystallization age from 630 to
319 480 Ma. This includes the Plutonic Central Domain of Mondou et al. (2012) and the Carlos
320 Chagas anatectic domain (Figs. 3 and 5 b-d), which is a 100 by 300 km large area
321 dominated by anatectic rocks formed by partial melting of the middle crust and deformed
322 predominantly at the magmatic state (Cavalcante et al., 2013). The Plutonic Central
323 Domain consists of tonalitic and granodioritic bodies (the “Galiléia” and “São Vitor”)
324 emplaced during a magmatic event at ~580 Ma and deformed at the magmatic state,
325 coherently with their metasedimentary country rocks (Mondou et al. 2012). These bodies
326 have calc-alkaline composition interpreted as representative of a magmatic arc, which
327 would span from 630 to 585 or 580 Ma (e.g., Tedeschi et al. 2016) and imply the
328 consumption of oceanic crust for 45-50 million years. Paragneisses showing evidence of
329 partial melting are widespread in the internal domain (blue unit 3 in Fig. 3), and are at least
330 in part considered to represent partially molten Macaúbas Group (e.g., Dias et al., 2016),
331 but also synorogenic metasediments (Nova Venécia Group; Richter et al., 2016).
332 Temperature estimates from different techniques consistently indicate peak metamorphic
333 temperatures of 750-850 °C for this internal core of the orogen (Cavalcante et al., 2014;

334 Moraes et al., 2015; Dias et al., 2016) and pressures around 6-7 kbar (Munhá et al., 2005;
335 Moraes et al., 2015). The abundant granitoid rocks in the hot internal orogenic domain have
336 been separated into (super)suites representing “pre-collisional” arc magmatism (630-580), a
337 “syn-collisional” (585-530 Ma) and a “post-collisional” (530-480 Ma) suite by Pedrosa-
338 Soares et al. (2001, 2011; Gonçalves et al. 2016). The “pre-collisional” suite (also called
339 G1) is dominated by I-type, metaluminous to slightly peraluminous expanded calc-alkaline
340 granites, while the “syn-collisional” (also called G2) granites mostly consists of S-type,
341 peraluminous, sub- to calc-alkaline granites (Gonçalves et al., 2014; Tedeschi et al., 2016).
342 Acceptance of this classification and evolutionary model poses important implications for
343 the tectonic and kinematic evolution of the Araçuaí-West Congo orogen, as will be
344 discussed in more detail below.

345

346 **4. How much shortening across the Araçuaí–West Congo orogen?**

347 In general, to estimate the amount of shortening between two converging continents
348 we need to consider both the contribution from oceanic consumption (subduction) and the
349 horizontal shortening and corresponding vertical thickening of the continental margin
350 during what is referred to as the continent-continent collision phase. We will start with the
351 shortening involved in the crustal thickening process, generally considered as the result of
352 continent-continent collision between the east margin of the São Francisco craton and the
353 west margin of the Congo craton.

354

355 *4.1 Shortening associated with the crustal thickening (“collision”)*

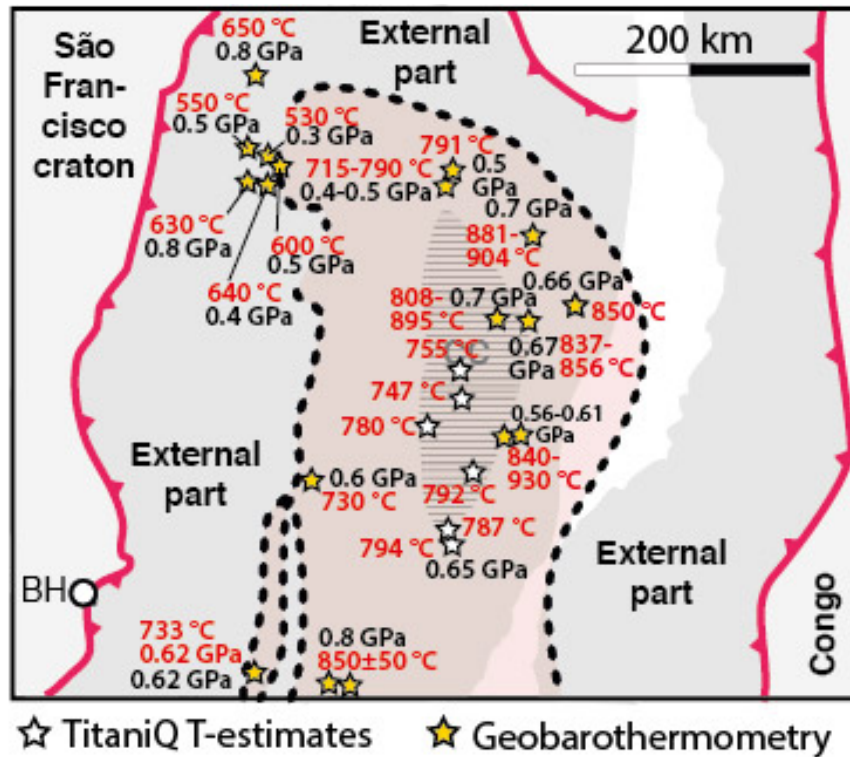
356 The relationship between crustal thickening and convergence is not always
357 straightforward at convergent plate boundaries. Vanderhaeghe and Duchêne (2010) have
358 shown how the pattern of thickening relates to slab advancement or retreat, and to the
359 degree of coupling between the mantle lithosphere and the overlying continental crust.
360 However, in a confined orogen such as the Araçuaí–West Congo, where there is no
361 evidence of deep subduction of continental crust and where continental accretion due to any
362 slab rollback would be balanced by upper-plate stretching, is a simpler case. In this case the
363 thickening of the continental crust is proportional to the horizontal shortening and
364 convergence between the southern São Francisco and West Congo parts of the Congo
365 craton during what is referred to as the collisional stage in the recent literature on this
366 orogen.

367 Estimating the amount of shortening of continental crust across orogens commonly
368 involves palinspastic reconstructions or section restorations. Such restorations are difficult
369 to perform for the Araçuaí–West Congo orogen because of the lack of restorable
370 allochthonous units (thrust nappes) and marker horizons, and poor depth control due to low
371 topographic relief and little relevant geophysical data. Furthermore, deformation in the
372 internal hot part of the orogen was disseminated and absorbed by partially molten rocks
373 with little memory of strain and displacement (Vauchez et al., 2007). Hence, the best
374 approach is to consider the transformation of thin, rifted crust to an overthickened orogenic
375 continental crust. This involves assumptions regarding the preorogenic basin and the
376 geometry and thickness of the resulting orogenic belt.

377 The proximal margins of the pre-orogenic Macaúbas basin are located under the
378 foreland fold-and-thrust belt on both the São Francisco and West Congo sides of the orogen

379 (Tack et al., 2001; Pedrosa-Soares et al., 2008) (Fig. 3). This implies that the orogenic
380 foreland closely coincides with the limits of the pre-orogenic volcano-sedimentary basin,
381 whose attenuated crust was subsequently shortened, metamorphosed and incorporated into
382 an orogenic crust that was thick and hot enough for extensive melting to occur.

383 The crustal thickness that was achieved during the Araçuaí–West Congo orogeny is
384 revealed by metamorphic pressure estimates. Pressure associated with the metamorphic
385 peak (ca. 580 Ma) have been calculated by several authors from different sections of the
386 internal part of the orogen, and most of the data indicate pressures of 0.6-0.7 GPa (Munhá
387 et al., 2005; Belém, 2006; Petitgard, 2009; Uhlein et al., 2009; Gradim et al., 2014;
388 Cavalcante et al., 2014; Moraes et al., 2015; Dias et al., 2016; Gonçalves et al., 2016), with
389 slightly higher pressures (~0.8 GPa) reported from the southernmost part of the Araçuaí
390 belt (Bentos dos Santos et al., 2011) (Fig. 6). These data indicate that the present erosion
391 level was located at depths of around 20-25 km during the metamorphic peak, and that the
392 crustal thickness in the internal part of the orogen was fairly constant, as expected for a
393 plateau-type orogen (Vanderhaeghe and Teyssier, 2001). With a uniform current crustal
394 thickness of around 40 km (Assumpção et al., 2017), this implies that the crust was fairly
395 flat-based with a total thickness of 60-65 km across the hot internal part of the orogen at the
396 time of peak Araçuaí–West Congo metamorphism (e.g., Cavalcante et al., 2014). Deep
397 crustal subduction not only produces roots, but also channels of vertical extrusion along
398 which (ultra)high pressure rocks are exhumed (Liou et al., 2004; Butler et al., 2013), and
399 we find no trace of such extrusion in the Araçuaí–West Congo orogen.



400

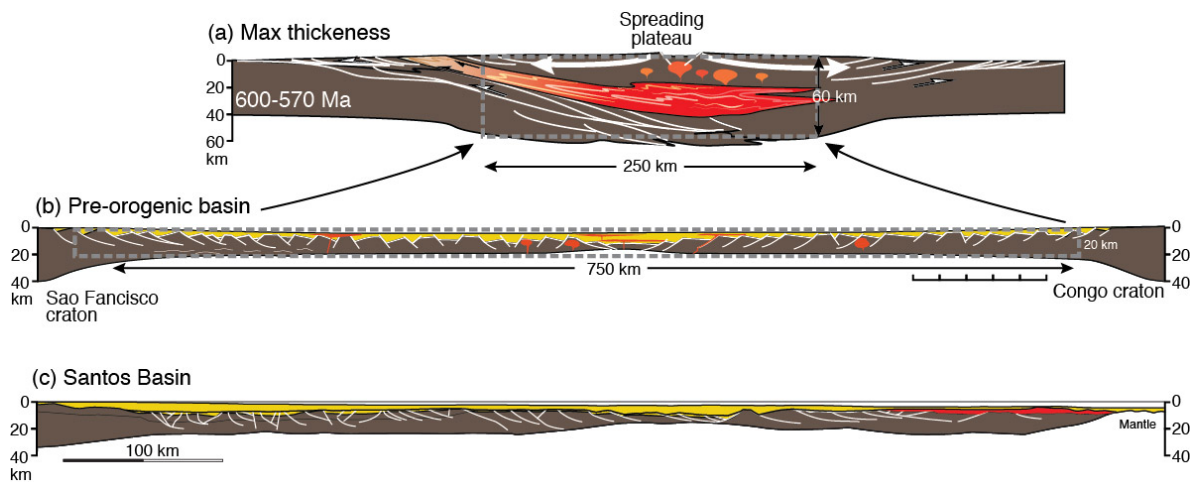
401 **Figure 6.** Peak pressure and temperature estimates from the internal hot part of the
 402 orogen. TitaniQ temperatures represent minimum crystallization temperatures of quartz
 403 from Cavalcante et al. (2014 and 2018). Geobarothermometric data from Garcia et al.
 404 (2003), Schmitt et al. (2004), Munhá et al. (2005), Belém (2006), Petitgirard et al. (2009),
 405 Uhlein et al. (2009), Bento dos Santos et al. (2011), Gradim et al. (2014), Moraes et al.
 406 (2015), Degler et al. (2018).

407

408 To estimate the pre-orogenic crustal thickness, we consider the current 40 km
 409 thickness of the São Francisco craton (Assumpção et al., 2017) to have been the cratonic
 410 thickness also in the Neoproterozoic. Furthermore, the pre-orogenic basin must have been
 411 wider than the ~600 km wide orogenic belt, and this continental crust was a rift or rifted
 412 margins with thinned crust. The crustal thickness in wide continental margin or rift settings
 413 is variable, but is usually around or slightly less than half of its original thickness (e.g.,

414 Faleide et al., 2008; Reston 2010; Huismans and Beaumont, 2014). Hence an average
 415 reduction from 40 to 20 km seems like a reasonable estimate. Basin sediments that were
 416 later metamorphosed during the orogeny and thus contributed to the Araçuaí–West Congo
 417 crust are included in this estimate, but any oceanic crust that might have existed is assumed
 418 to have been subducted and is therefore not considered.

419 Using this assumption, the hot internal part of the orogen increased in thickness from
 420 20 to 60 km over its current width of ~250 km (Fig. 7a) during the orogeny. Restoring to a
 421 pre-orogenic basin with 20 km crustal thickness gives a 750 km wide basin and 500 km of
 422 orogenic shortening, as illustrated schematically in Fig. 7b. For comparison, a 750 km wide
 423 continental basin is similar to the rifted South Atlantic margin across the Santos basin (Fig.
 424 7c) (e.g., Szatmari and Milani, 2016), and the width of the Basin and Range basin in the
 425 western USA is around 800 km.



426

427 **Figure 7.** a) Schematic cross-section through the Araçuaí orogen at the time of partial
 428 melting of the middle crust. b) Illustration of what the pre-orogenic Macaúbas basin may
 429 have looked like. An average Moho depth of 20 km is chosen. Stippled rectangle in a)
 430 reflects the average crustal thickness in the thick-skinned part of the orogen, and the
 431 corresponding pre-orogenic shape of this area is presented by the rectangle in b). c) The

432 *800 km wide rifted South Atlantic margin across the Santos basin, for comparison (from*
433 *Magnavita, 2014 and Szatmari et al., 2016).*

434

435 In addition, some foreland shortening outside the rectangular area in Fig. 7 occurred,
436 but at least some of this foreland thrusting/thickening was driven by gravitational spreading
437 of the internal part of the orogen after peak metamorphism, and this part should not be
438 included. More dating of deformation in the foreland is necessary to distinguish between
439 these two components. On the contrary, any material added or subtracted to the section by
440 northward flow from the pinching point at the southern termination of the São Francisco
441 craton would affect the amount of shortening to some extent. Similarly, introduction of
442 intrusive rocks from the mantle during the orogeny would overestimate the amount of
443 thickening. However, most of the magmatic rocks originated by partial melting of the crust
444 (Gonçalves et al., 2017) and would therefore not affect the mass balance. Hence, our 500
445 km estimate of orogenic shortening is considered to be a reasonable first-order estimate.

446 According to most recent workers the Araçuaí–West Congo orogeny lasted for 50-55
447 m.y. (585-530 Ma) (Pedrosa-Soares, 2001, 2011; Gradim et al., 2014; Tedeschi et al., 2016;
448 Alkmim, 2017). The convergence rate during continent collision is usually considerably
449 lower than those typical for oceanic subduction, because of the gravitational resistance of
450 continental crust to subduction. For instance, the convergence rate of the Himalayan system
451 slowed down from >10 cm/y to 4.5 cm/y (Klootwijk et al., 1992). For a confined situation
452 like the Araçuaí–West Congo orogen, the convergence may have been even slower. For
453 example, a low average convergence rate of 1 cm/y would, over 50 m.y., produce 500 km

454 of shortening across the Araçuaí-West Congo orogen, i.e. the same order of magnitude
455 estimated above.

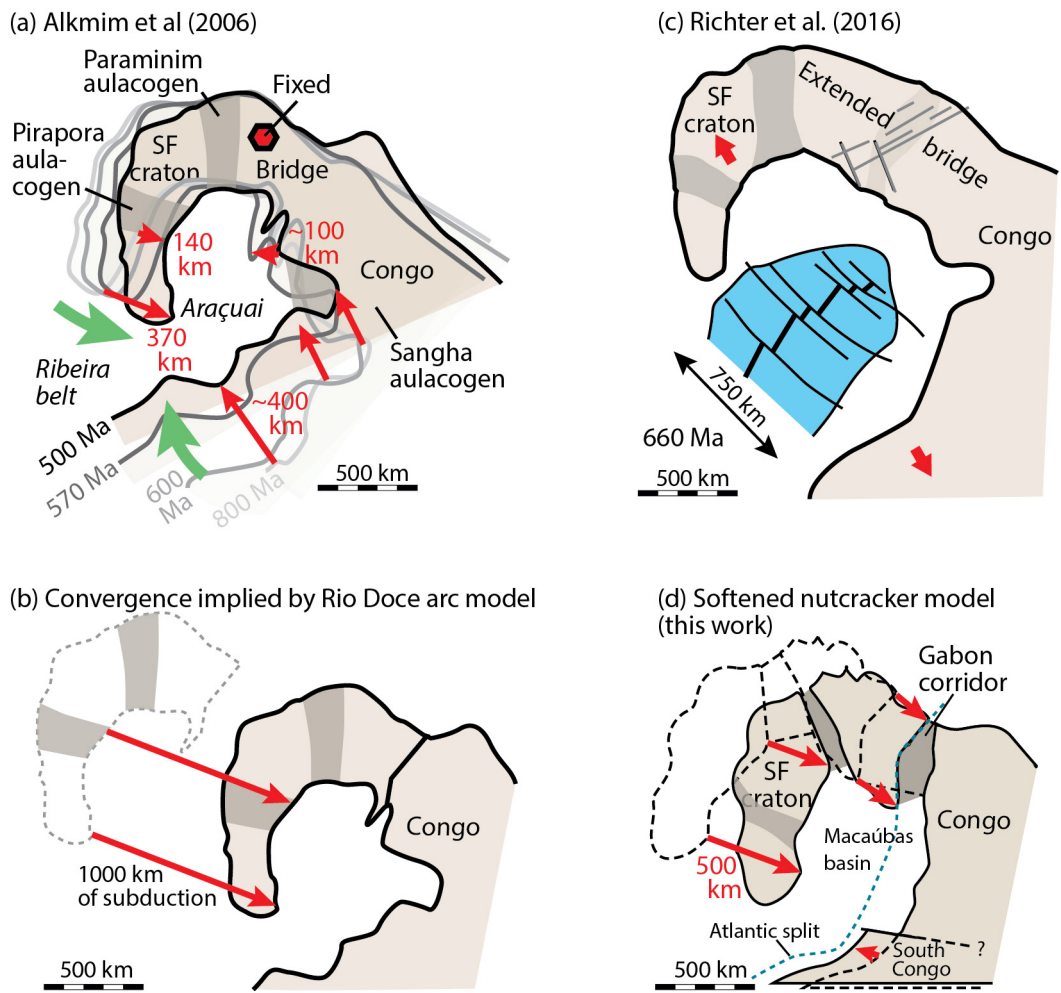
456

457 *4.2 Implications of any “pre-collisional” subduction*

458 Any subduction of oceanic crust prior to what is referred to as “collision” in the
459 recent literature would imply convergence prior to the continental shortening discussed
460 above. The prevailing model regarding oceanic crust in the Macaúbas basin and its
461 consumption involves extensive arc magmatism and prolonged subduction of oceanic crust
462 (Pedrosa-Soares et al., 2011; Gonçalves et al., 2014), as presented or assumed in a large
463 number of recent contributions (e.g., Pedrosa-Soares et al., 1998, 2001, 2008; Alkmim et
464 al., 2006; Gradim et al., 2014; Kuchenbecker et al., 2015; Moraes et al., 2015; Peixoto et
465 al., 2015; Dias et al., 2016; Gonçalves et al., 2016, 2017; Richter et al., 2016; Tedeschi et
466 al., 2016; Alkmim et al., 2017; Degler et al., 2017; Melo et al., 2017a, b). This model is
467 based on geochemical and geochronologic data from magmatic rocks in the orogen, and
468 argues for ~50 m.y. of arc magmatism and related subduction of oceanic crust. Subduction
469 rates generally vary from 2-10 cm/y, for example the fast subduction of the oceanic part of
470 the Indian plate under Asia at >10 cm/y (prior to the Himalayan collision) versus the slow
471 subduction at ~2 cm/y for the Lesser Antilles system (Stein, 1983). Picking a slow
472 subduction rate of 2 cm/y implies ~1000 km of shortening across the Macaúbas basin prior
473 to continent collision. This most likely represents about ~1000 km of eastward
474 displacement of the São Francisco craton relative to the Congo craton. Arguably, slab
475 rollback could absorb a limited amount of these 1000 km by further stretching of an already
476 thinned continental margin. At some point slab rollback would create an oceanic back-arc

477 basin that would produce new oceanic crust. Regardless, the unsolvable problem of putting
478 a 1000 km wide ocean into the confined environment of the Araçuaí-West Congo remains.
479 An ocean close to this size (750 km) was schematically indicated by Richter et al. (2016)
480 (Fig. 8c). However, by adding such an ocean to this embayment leaves far too little
481 continental margin to even thicken the crust to normal thickness, let alone to build a 60-65
482 km thick orogenic crust, as shown in Fig. 7.

483 Other references to the size of this ocean have been made by Pedrosa-Soares et al.
484 (1998), who state that “the extensive occurrence of syntectonic to late tectonic calc-alkalic
485 granitoids along the internal domain of the Araçuaí belt implies that a reasonably large
486 amount of ocean crust was consumed”. As discussed above, “reasonable” implies
487 something in the order of 1000 km or more. However, in another publication Pedrosa-
488 Soares et al. (2001) state that “only a narrow oceanic lithosphere was generated, and it was
489 subducted afterwards”. Such self-contradictory statements illustrate the need for
490 quantitative evaluations when considering tectonic models for the Araçuaí-West Congo
491 orogen.



492

493

494 **Figure 8.** a) Evolution of the confined Araçuaí orogen as interpreted by Alkmim et al.
 495 (2006, their fig. 15), showing progressive closing of the pre-orogenic Macaúbas basin at
 496 800, 600, 570, and 500 Ma (successively less transparent). b) Restoration of the São
 497 Francisco craton to allow for a 1000 km wide ocean between the São Francisco and Congo
 498 cratons that was subducted during convergence. Note that the crustal thickening
 499 (“collisional phase”) implies additional 500 km of displacement. c) Model presented by
 500 Richter et al. (2016), where an ocean has been allowed by extending the continental bridge
 501 considerably. Richter et al. provide no explanation for how this bridge shortened during
 502 the orogeny. d) Modified model, taking into account the Gabon corridor, here considered
 503 to accommodate ~200 km of orthogonal shortening.

504

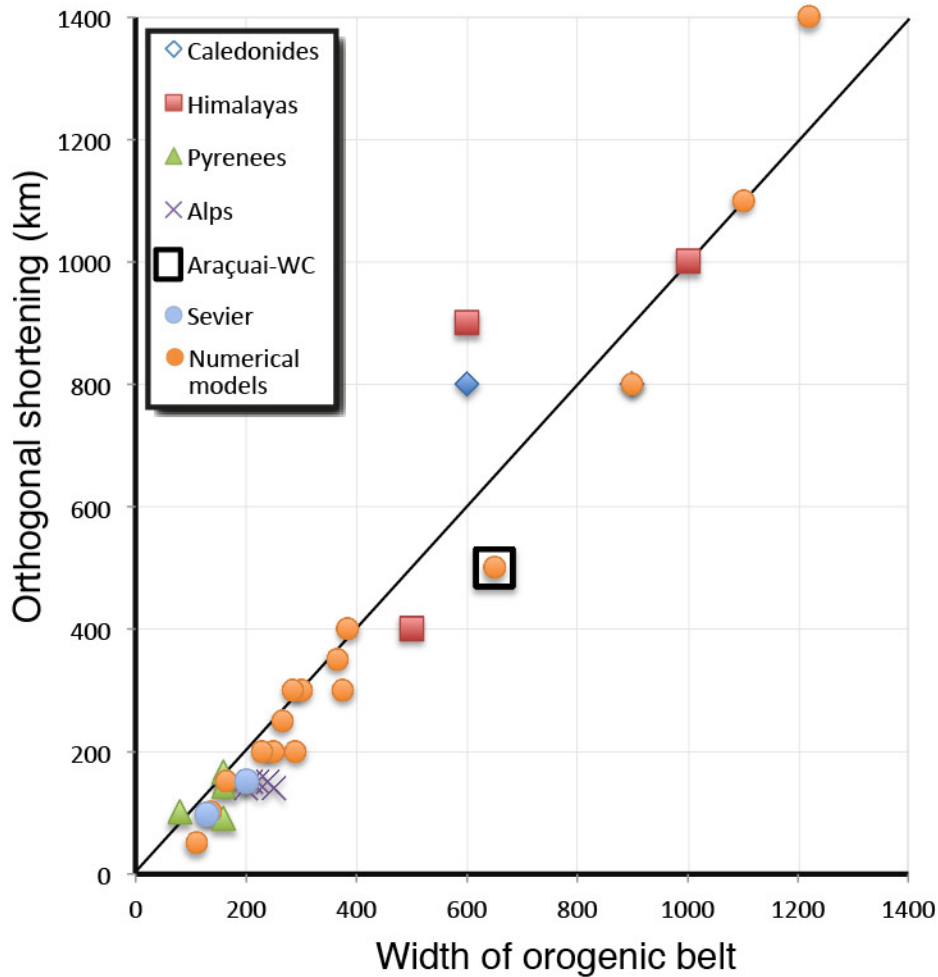
505 **5. Kinematic models for the Araçuaí-West Congo orogen**

506 The above discussion suggests that ~500 km of convergence is needed to form the
507 Araçuaí-West Congo orogen in an intracontinental setting, and that additional convergence
508 on the order of 1000 km is needed to explain the widely published model of extensive arc
509 magmatism. In the following we will discuss the implications of these numbers in terms of
510 the constraints imposed by the confined orogenic setting.

511 The kinematic evolution of the Araçuaí-West Congo orogen has been discussed
512 qualitatively by Alkmim et al. (2006), who presented the “nutcracker” model where the
513 Macaúbas basin and its underlying crust were shortened by anticlockwise rotation of the
514 São Francisco craton relative to Congo (indicated by green arrows in Fig. 8). Figure 8a
515 shows successive stages of Alkmim et al.’s model, from 800 Ma (pre-convergence) until
516 the post-orogenic stage (500 Ma). This presentation shows that their model, based on their
517 own illustration, produces only ~300 km of total convergence across the central Araçuaí
518 part of the orogen, decreasing to the north and increasing to ~750 km at the southern
519 termination of the São Francisco craton and into the Ribeira belt. Hence, this model has
520 difficulties accounting for the crustal thickening associated with the Araçuaí-West Congo
521 orogen, and has no room for any oceanic crust at all.

522 To illustrate the problems involved in incorporating the >1000 km of estimated
523 subduction-related shortening, the São Francisco craton was moved 1000 km to the west in
524 Fig. 8b. This amount of convergence would require the São Francisco craton to have moved
525 completely independent of the Congo craton, which is incompatible with the nutcracker
526 model and the idea of a cratonic bridge, as discussed above. In an apparent attempt to get

527 around this problem, Richter et al. (2016) in their reconstruction (their figure 2) extended
528 the bridge connecting the São Francisco and Congo cratons. Richter et al. (2016) provide
529 no explanation as to how their shortening of this part of the craton was accommodated.
530 However, we have already pointed out that the Gabon corridor (Fig. 8d) could
531 accommodate such strain, but how much? This corridor is 150–200 km wide (depending on
532 the interpretation and restoration of the passive margins in the area), and based on the
533 global relationship between width and shortening across orogenic belts (Fig. 9) it seems
534 unlikely to represent much more than 200 km of orthogonal shortening. Further, there is not
535 room for any significant additional strike-slip deformation along the Gabon corridor, as
536 such motions would be hampered by the transverse Sergipano belt to the north. A
537 reconstruction similar to the one by Alkmim et al. (2006), but with the Gabon corridor
538 added, allows for a total of ~500 km of shortening across the Araçuaí-West Congo orogen.
539 This may be sufficient to explain the crustal thickening reflected by the geobarometric data,
540 but it leaves no space for the subduction-related consumption of oceanic crust called for in
541 most recent publications from this orogen (e.g., Pedrosa-Soares et al., 1998). In other
542 words, the combined strain associated with the Gabon corridor, Paramirim aulacogen and
543 other structures that split the craton into subunits cannot allow for much more than 500 km
544 of convergence across the Araçuaí-West Congo orogen.
545



546

547 **Figure 9.** Width of orogenic belts plotted against their orthogonal shortening, based on
 548 data from Armstrong, 1968; Beaumont et al., 2000, 2010; DeCelles and DeCelles 2001,
 549 2002; Erdős et al., 2014; Long et al., 2011; Li et al, 2015; Mouthereau et al., 2014;
 550 Robinson and Delores, 2008; Rosenberg and Berger, 2009; Schmid and Kissling, 2000;
 551 Weil and Yonkee, 2012. The reference line indicates a linear 1:1 relationship between
 552 orthogonal shortening and orogenic width.

553

554 We conclude that qualitatively, the “nutcracker” model by Alkmim et al. (2006) is a
 555 viable model, but that it needs some additional flexibility to accommodate the strain
 556 associated with the mountain building. We suggest that this flexibility can be added along

557 the orogenic zone extending northward across the bridge along the current Atlantic margin.
558 Furthermore, it is clear that the arc development presented in the literature is at odds with
559 even the softened nutcracker model (Fig. 8d) or any other kinematic model proposed for the
560 region (see Alkmim et al., 2006 for a review), and we raise the question if there was ever
561 any significant amount of oceanic crust in this northern part of the Mantiqueira orogenic
562 province.

563

564 **6. Was there an ocean at all?**

565 *6.1 Possible ophiolite fragments*

566 The possibility that the pre-orogenic Macaúbas basin rested on extended continental
567 crust with no significant amount of oceanic crust has been advocated by Trompette (1994;
568 2000) and later by Meira et al. (2015), who suggested the entire Ribeira–Araçuaí orogen to
569 be intracratonic. Contrary to this interpretation, restricted occurrences of amphibolites
570 (interpreted as metabasalt) and metamorphosed ultramafic rocks have been presented as
571 evidence of oceanic crust from the pre-orogenic basin (Pedrosa-Soares et al., 1998). In
572 general, orogens that involve tens of millions of years of subduction and island arc activity,
573 such as the Caledonides, Appalachians and the Himalayas all contain abundant evidence of
574 oceanic crust in the form of well preserved ophiolite complexes, in addition to island-arc
575 magmatism, even if we consider a high grade of chemical weathering. It is also worth
576 noting that several ophiolites in the Alpine orogenic system have been suggested to be rift-
577 or breakup-related, and not actual oceanic crust (Koglin et al., 2009; Dilek and Furnes,
578 2014). Hence, ophiolite fragments are not evidence for a former oceanic basin.

579 In the Araçuaí-West Congo orogen, the possible ophiolite fragments are small,
580 strongly altered, do not display any characteristic ophiolite pseudo-stratigraphy, bear no
581 information about the extent of oceanic crust, except that they are claimed to be almost 200
582 m.y. older than the early magmatism that is interpreted as arc magmatism and subduction
583 initiation (Pedrosa-Soares et al., 1998). This is a very long time span (for comparison,
584 nearly all current oceanic crust is younger than 200 m.y.) and would imply a several
585 thousand kilometers wide pre-orogenic ocean, comparable in width to that of the Atlantic
586 Ocean. Subducting such a wide ocean over 50 m.y. (630-580 Ma) is another challenge in a
587 confined system such as the Araçuaí-West Congo. Furthermore, it is unusual in any orogen
588 to preserve such old and dense oceanic crust. Instead, most orogenic ophiolites represent
589 buoyant oceanic crust from small and young oceanic forearcs or backarcs basins (Stern,
590 2004).

591 There are several examples of orogens that only involved very small oceanic basins
592 or no oceanic crust at all. The Alps is a well-known example, and it still contains ophiolitic
593 rocks (e.g., Chenin et al., 2017). The Pyrenean orogen is another example where oceanic
594 crust may not have been involved at all (Beaumont et al., 2000). Instead, a domain of
595 hyperextended continental crust and extended subcontinental depleted mantle appears to have
596 existed. Whether this was the case in the Macaúbas rift basin is unknown, but should be
597 kept in mind.

598

599 *6.2 Orogenic magmatism*

600 The interpretation of large paleo-oceans in convergent settings typically relates to
601 long-lived arc magmatism, identified by tectonic context and geochemical and isotopic
602 signature. While a review of the vast amount of published geochemical data from the
603 Araçuaí-West Congo orogen is outside of the scope of the present contribution, we note
604 that magmatic rocks considered to represent a pre-collisional arc (Rio Doce arc; Tedeschi et
605 al., 2016) was built upon Paleoproterozoic continental crust considered to represent the
606 western margin of the Congo craton (Gonçalves et al., 2017). Even though some these early
607 magmatic rocks share geochemical similarities with rocks from more modern continental
608 arcs, for instance the Sierra Nevada arc and the Andean belt (Gonçalves et al., 2014, 2016),
609 distinguishing between arc-generated magmatic rocks and magmatic rocks formed during
610 hot continental orogenesis is not straight-forward (e.g., Barbarin, 1999). More specifically,
611 the calc-alkaline composition of magmatic rocks from the central domain of the Araçuaí
612 belt (Galiléia and São Vitor bodies) is not unequivocal evidence for subduction-related
613 magmatic arcs, as suggested by Tedeschi et al. (2016). Such a composition can also be
614 found in extensional settings, such as the Basin and Range province (Western USA) and the
615 Gulf of California (e.g., Sheth et al. 2002) and in continental collision settings (e.g.,
616 Barbarin 1999). It also seems relevant in this context to point out that the basement to the
617 Ediacaran Rio Doce magmatic rocks was already a juvenile Early Proterozoic magmatic
618 arc, based on its geochemical signature, ϵ Nd values and the absence of inherited zircon
619 grains (Noce et al. 2007). Hence the origin and tectonic implications of the 630-575 Ma
620 magmatism in the Araçuaí belt should be critically reassessed, as already suggested by
621 Meira et al. (2015).

622

623 **7. A revised orogenic model**

624 Concluding from the above that any pre-orogenic ocean must have been very small or
625 absent, we would expect orogenic thickening between the two cratonic margins to have
626 happened at a much earlier time than that postulated by most authors (585-580 Ma;
627 Pedrosa-Soares, 2001, 2011; Gradim et al., 2014; Tedeschi et al., 2016; Alkmim, 2017).
628 New radiometric and thermal data show that crystallization of the anatectic core of the
629 orogen (Carlos Chagas anatectic domain) was going on already around 600 Ma, and that
630 the middle crust at this point was already heated to more than 750 °C in a large (150,000
631 km²) area (Fig. 6) (Cavalcante et al., 2018). The achievement of such high temperatures and
632 associated widespread partial melting together with the transformation of a thinned crust to
633 an overthickened orogenic crust requires time (~20 m.y.; e.g., Horton et al., 2016) (see
634 below). Hence, thickening of the continental crust could well have started at 630-620 Ma.
635 This eliminates the model involving prolonged subduction of a vast amount of oceanic
636 crust. Hence these two lines of arguments (little or no oceanic subduction, and crustal
637 thickening starting at 630-620 Ma) go very well together, and form the basis for an
638 alternative, hot orogen model for the Araçuaí-West Congo orogen.

639

640 Below we outline a hot orogen model for the Araçuaí–West Congo orogen that conforms to
641 the following conditions:

- 642 1) The total amount of convergence across the orogen was on the order of 500 km;
643 2) Only limited or no oceanic crust existed;

- 644 3) Much of the melt in the hot internal part of the orogen formed by partial melting
645 of the middle crust, probably in response to orogenic thickening and radioactive
646 decay;
- 647 4) Crustal thickening initiated earlier than 600 Ma, and probably before 620 Ma.

648

649 The first two points relate to the space problem involved in putting an ocean of any
650 significant size into the confined Araçuaí–West Congo orogenic system (Fig. 8) and are
651 already discussed above. The third point relates to evidence in favor of orogenic extrusion
652 or channel flow in a hot overthickened crust, as presented by Cavalcante et al. (2013, 2014,
653 2016), and the fourth point is based on recent dating of the crystallization of mid-crustal
654 melt in the central anatexitic part (Carlos Chagas anatexite) of the orogen (Cavalcante et al.,
655 2018).

656

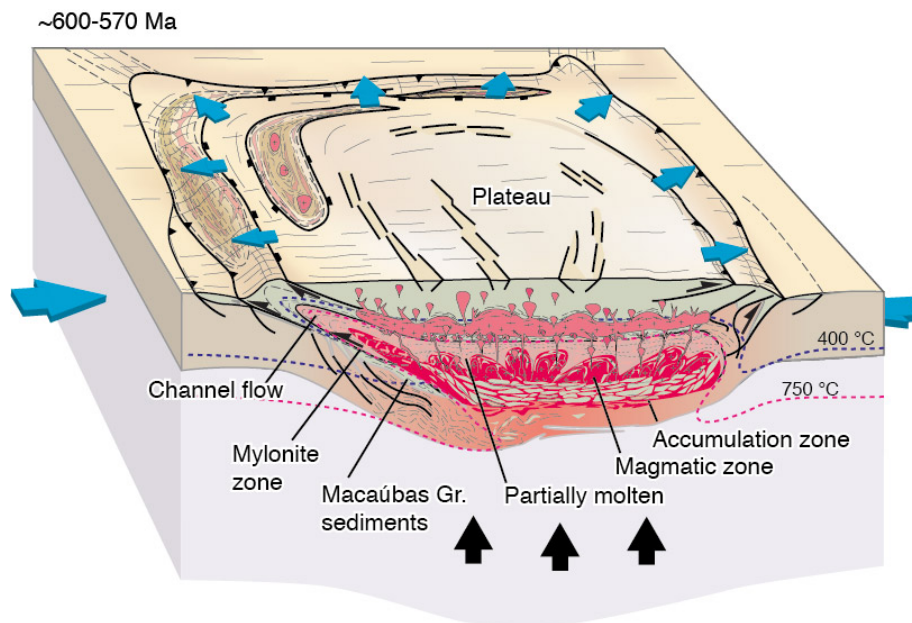
657 *7.1 The hot orogen model*

658 A hot orogen model for the Araçuaí–West Congo orogen has developed over the last
659 decade through the work by Vauchez et al. (2007), Petitgirard et al. (2007), Mondou et al.
660 (2012) and Cavalcante et al. (2013, 2014, 2018), and has implications for the temporal and
661 rheologic evolution of the Araçuaí–West Congo orogen that fits the kinematic constraints
662 of this orogen quite well (Fossen et al., 2017). Elevated temperatures in the central part of
663 the orogen may have several causes. One may be the high thermal gradient that can be
664 expected for the pre-orogenic rift. The radial arrangement of rift arms centered at the
665 location of the Araçuaí–West Congo orogen may indicate high heat flow from the mantle
666 during the pre-orogenic rifting. Hence the crust may have been hot already at the onset of

667 crustal thickening. The extensive magmatism governing the Araçuaí–West Congo
668 hinterland (Pedrosa-Soares et al., 2011) also suggests anomalously high temperatures in
669 this region both prior to, during and after the orogeny.

670 Furthermore, several lines of evidence suggest that elevated temperatures in this
671 orogen also relate to heat production by radiogenic decay of fertile sediments buried
672 (subducted) during the orogenic crustal thickening. One is the fact that melting occurred in
673 the middle crust at 20-25 km depth, which favors a mid-crustal heat source. Another is the
674 large volumes of potentially fertile sedimentary rocks in the Macaúbas basin, and the
675 observation that large amounts of peraluminous melt was produced from metasedimentary
676 midcrustal rocks, for instance in the Carlos Chagas anatectic domain (Cavalcante et al.,
677 2013). In general, heat production by radiogenic decay of buried sedimentary rocks in
678 collision zones leads to high temperatures (≥ 700 °C) in substantial volumes of the middle
679 crust after ~20 m.y. of collision (England and Thompson, 1986; Jamieson et al., 1998;
680 Sandiford and McLaren, 2002; Faccenda et al., 2008), generating a hot orogen with
681 associated profound crustal weakening (Vanderhaeghe, 2009; Jamieson and Beaumont,
682 2013). This is the scenario suggested for the crust underlying the Tibetan plateau (Nelson et
683 al., 1996; Vanderhaeghe and Teyssier, 2001; Zhang et al., 2004), where the present crustal
684 thickness is at least doubled, where middle to lower crustal temperatures are well above
685 700 °C (Klemperer, 2006), and where melting started some 20-25 m.y. after the collision
686 and is still ongoing 30 million years later (Jamieson et al., 2011). A schematic illustration
687 of such an orogenic evolution is shown in Figure 10. Transferred to the Neoproterozoic
688 Araçuaí–West Congo orogen where melting was ongoing at around 600 Ma (Cavalcante et
689 al., 2018), this implies that orogenic thickening started before 620 Ma. Recent dating of

690 recrystallization of detrital zircon at ~630-625 Ma in metasedimentary rocks in the
691 Macaúbas basin, interpreted as a regional metamorphic event in a convergent regime
692 (Schannor et al., 2018) is consistent with such a model.



693
694 **Figure 10.** Idealized illustration of the formation of a hot orogen at the time of maximum
695 crustal thickness with extensive partial melting, where the molten crust is starting to flow
696 toward the foreland (channel flow) which again leads to plateau uplift and exhumation of
697 the lower crust (black arrows). Modified from Vanderhaeghe (2009).

698
699 The Variscan and Grenville orogens represent ancient examples explained by similar
700 processes (Vanderhaeghe et al., 1999; Turlin et al., 2018), and both the Variscan, Grenville
701 and Himalayan orogens show evidence of lateral channel flow or extrusion (Fig. 4) of mid-
702 crustal material under a stronger upper crust that stretched during slow gravity-driven
703 orogenic spreading. This model fits the Araçuaí–West Congo orogen and its high
704 temperatures and extensive partial melting, and estimates of temperature and magma
705 viscosity from the anatectic part of the Araçuaí orogen (Cavalcante et al., 2014). Important

706 evidence of flow of partially molten middle crust is based on structural mapping based on
707 outcrop observations and magnetic fabrics determined by the AMS (Anisotropy Magnetic
708 Susceptibility) method in the anatectic core of the orogen (Carlos Chagas anatectic domain;
709 Cavalcante et al., 2013). This work shows a magmatic-state middle crustal flow pattern
710 consistent with gravitational collapse of the upper and middle crust and the more or less
711 radial top-to-foreland kinematics shown in Fig. 3. In this scenario gneiss domes tend to
712 form, as seen in eroded hot orogenic belts as well as in numerical models of hot orogenic
713 settings (e.g., Vanderhaeghe and Teyssier, 2001; Rey et al., 2009, 2010). The fluctuating
714 structural pattern of mostly low-angle fabrics in the anatectic parts of the Araçuaí orogen
715 presented by Cavalcante et al. (2013) is consistent with deep sections through the roots of
716 such core complexes (e.g., Vanderhaeghe, 2009). Channel flow would also cause northward
717 flow of high-grade rocks toward the São Francisco foreland (the bridge region), explaining
718 the relatively short distance between the hot core of the orogen and its northern termination
719 (Figs. 3 and 6). We do not see evidence for vertical extrusion of light lower crustal hot and
720 partially molten material, such as suggested for the Variscan orogen by Schulmann et al.
721 (2008, 2014). Such overturning produces steep foliation and lineation patterns overprinted
722 by low-angle fabrics related to subsequent lateral extrusion, while the hot central part of the
723 Araçuaí-West Congo belt exhibits low-angle fabrics and in-situ middle-crustal melting.
724 Some melt is likely to have come from the lower crust and the mantle, but the majority of
725 melt at the present mid-crustal erosion level appears to have formed within the middle
726 crust, since we do not observe any intrusive relationships (Cavalcante et al., 2013).

727 Plateau collapse related to lateral flow of the middle crust from ~600 Ma implies the
728 existence of an extending upper crustal orogenic lid that is now removed by erosion. Some

729 of the upper crust is preserved in the Ribeira and Dom Feliciano belts to the south, where a
730 system of middle Ediacaran (~600 Ma) to early Cambrian rifts have been mapped (Almeida
731 et al., 2010, 2012). A collapsing hot orogen model provides a viable explanation for the
732 formation of these upper crustal rift basins, and this situation is consistent with the constant
733 crustal thickness reflected by P-T data (Fig. 6).

734

735 **8. Final discussion and concluding remarks**

736 The partly confined geometry of the Araçuaí–West Congo orogen limits the amount
737 of shortening across the orogen to maximum ~500 km, excluding models that call for ~50
738 m.y. of arc magmatism and associated subduction of oceanic crust. Instead, a hot orogenic
739 model is favored, where heating during crustal thickening contributed to extensive partial
740 melting from ~600 Ma, implying initiation of crustal thickening before 620 Ma. This is
741 close to the time (~630 Ma) of collisions along the north, west and south margins of the São
742 Francisco craton (Fig. 2), which probably caused the shortening of the Macaúbas basin that
743 lead to the formation of the Araçuaí–West Congo orogen. The hot orogeny model outlined
744 above involves internal heat production by radiogenic decay of buried rocks and sediments.
745 Crustal heat production from radioactive elements (U, Th, K) can be a sufficient source of
746 heat for partial melting of thickened continental crust (Jamieson et al, 1998; Sandiford and
747 McLaren, 2002; Faccenda et al., 2008), combined with heating of the system during the
748 pre-orogenic stretching of the crust across the Macaúbas rift basin. A syn-orogenic mantle
749 heat source has also been suggested by several authors (Gradim et al., 2014; Bento dos
750 Santos, 2015; Tedeschi et al., 2016). Regardless, explaining extensive magmatism and
751 partial melting of crustal material by prolonged island arc development is incompatible

752 with the confined nature of this orogen. In contrast, the hot orogen model can explain much
753 of this melt generation within a framework of a softened nutcracker model. Such a model
754 has been successfully used to explain other orogens, including the Himalayas, Grenville
755 and Variscan orogens (Beaumont et al., 2010; Jamieson et al., 2011).

756 The ~500 km of shortening estimated across the orogen occurred during the first and
757 main part of the orogenic history, until extensive partial melting was established at ~600
758 Ma (Cavalcante et al., 2018). Once extensive melting of the middle crust was established,
759 slow collapse of the central parts of the orogen may have driven thrusting toward the
760 foreland, at least until 570 Ma, which is the youngest age of melt crystallization reported
761 from the anatectic core (Cavalcante et al., 2018). However, evidence of younger orogenic
762 activity has been reported. For example, the Três Marias Formation, which contains 558
763 Ma old detrital zircons (Kuchenbecker et al., 2015; Alkmim et al., 2017), has been involved
764 in thrusting. Furthermore, the age of the youngest syn-kinematic intrusive body dated in the
765 Araçuaí belt is ~530 Ma (the Ibituruna syenite; Petitgard et al., 2009), whereas the oldest
766 post-kinematic granite is ~520 Ma (Noce et al., 2000). These observations may indicate a
767 young pulse of orogeny, possibly related to the ~540 Ma Cabo Frio orogeny reported from
768 the eastern Ribeira belt and the southernmost West Congo belt (Schmitt et al., 2016; Monié
769 et al., 2012). Continuous orogenic convergence for ~100 m.y. is considered unlikely, as it
770 would accumulate too much shortening. We suggest that late-orogenic thrusting driven by a
771 collapsing hot central part of the orogen should be further considered as more data
772 accumulate.

773 To understand this unusual termination of a large orogenic belt in a confined cratonic
774 environment requires dedicated and high-quality dating of melt crystallization in a wider

775 part of the hinterland. Such data should be compared with results from direct dating of
776 thrusting in the low-temperature foreland fold-and-thrust belt, for example by Ar/Ar dating
777 of micas grown below the retention temperature (Oriolo et al., 2018 and references therein).
778 Furthermore, better mapping of the thermal structure of the orogen and numerical modeling
779 of both the thermal and kinematic aspects discussed in this paper would be beneficial, and
780 orogenic strain should be estimated across the reactivated Paramirim aulacogen. A better
781 separation of the pre-orogenic rift sequence and the syn-orogenic deposits would also
782 enhance our understanding of the orogenic evolution. Finally, the geochemical aspects of
783 the various melts and magmatic rocks in the orogen require closer attention to explore
784 alternatives to a conventional magmatic arc interpretation, since there is an overlap between
785 the crystallization ages of the Galiléia and São Vitor bodies (Rio Doce magmatic arc; 580
786 Ma) and the Carlos Chagas anatexite (~600-570 Ma). Several fundamental implications of
787 the kinematic constraints of this orogen are pointed out here, but there is a need for critical
788 evaluation of both data and models, and there is also a general lack of quantitative
789 structural considerations in the existing literature. Future work with this in mind will
790 undoubtedly reveal new details about this intriguing part of the Brasiliano/Pan-African
791 orogenic system. The main conclusions that we have been able to draw from the currently
792 available data are as follows:

793 -A non-rigid cratonic model along the lines presented by Alkmim et al. (2006) is
794 qualitatively viable only if loosened up by an orogenic corridor that breaks the “cratonic
795 bridge” between the São Francisco and Congo cratons.

796 -This softened nutcracker model is at odds with the widely published idea of 50 m.y.
797 of subduction-related arc magmatism in the Araçuaí–West Congo orogen, which should be
798 reconsidered.

799 -Our “softened nutcracker model” can only accommodate ~500 km of orogenic
800 shortening, which is required to form the 60-65 km thick orogenic crust.

801 -This hot orogen involves extensive partial melting of the middle crust, explainable
802 by radiogenic decay of fertile sediments and crustal heating during pre-orogenic
803 lithospheric thinning.

804 -Its extensively molten middle crust is likely to have produced foreland-directed
805 gravity-driven flow (spreading) that influenced foreland deformation. Hence, late foreland
806 thrusting does not necessarily directly reflect convergence but also relates to plateau
807 collapse.

808 -There is a need to better constrain the timing of deformation in the orogen by
809 geochronologic methods, particularly the low-temperature foreland deformation.

810

811 **Acknowledgments**

812 This work was supported by FAPESP projects 2015/23572-5, 2014/10146-5
813 2013/19061-0 and 2010/03537-7, and by the strong incentive for Brazilian research and the
814 public universities by former presidents Luiz Inácio Lula da Silva and Dilma Rousseff.
815 Additional support was provided by the Meltzer Research Fund (University of Bergen). CC
816 greatly appreciates discussions with Alain Vauchez, which introduced her into the hot
817 orogen model during her PhD research. Reviews by Olivier Vanderhaeghe and an
818 anonymous reviewer are greatly appreciated.

820 **References**

- 821 Alkmim, F.F., Kuchenbecker, M., Reis, H.L.S., Pedrosa-Soares, A.C., 2017. The Araçuaí belt. In:
822 M. Heilbron et al. (eds.), São Francisco Craton, Eastern Brazil, Regional Geology Reviews.
823 Springer International Publishing: 255-276.
- 824 Alkmim, F.F., Marshak, S., Pedrosa-Soares, A.C., Peres, G.G., Cruz, S.C.P., Whittington, A.,
825 2006. Kinematic evolution of the Araçuaí-West Congo orogen in Brazil and Africa:
826 Nutcracker tectonics during the Neoproterozoic assembly of Gondwana. *Precambrian*
827 *Research*, 149: 43-64. doi:10.1016/j.precamres.2006.06.007
- 828 Almeida, R.P., Janikian, L., Fragoso-Cesar, A.R.S., Fambrini, Gelson L., 2010. The Ediacaran to
829 Cambrian Rift System of Southeastern South America: Tectonic Implications. *The Journal*
830 *of Geology*, 118: 145-161. doi:10.1086/649817
- 831 Almeida, R.P., Santos, M.G.M., Fragoso-Cesar, A.S.R., Janikian, L., Fambrini, G.L., 2012.
832 Recurring extensional and strike-slip tectonics after the Neoproterozoic collisional events in
833 the southern Mantiqueira province. *Anais da Academia Brasileira de Ciências*, 84: 5-8.
- 834 Alvarez, P. 1995. Evidence for a Neoproterozoic carbonate ramp on the northern edge of the
835 Central African craton: relations with Late Proterozoic intracratonic troughs. *Geologische*
836 *Rundschau* 84, 636-648.
- 837 Araujo, C.E.G., Weinberg, R., Cordani, U., 2013. Extruding the Borborema Province (NE-Brazil):
838 a two-stage Neoproterozoic collision process. *Terra Nova*, 26: 157-168.
839 doi:10.1111/ter.12084
- 840 Archanho, C.J., Viegas, G., Hollanda, M.H.B.M., 2013. Timing of the HT/LP transpression in the
841 Neoproterozoic Seridó Belt (Borborema Province, Brazil): Constraints from U/Pb
842 (SHRIMP) geochronology and implications for the connections between NE Brazil and
843 West Africa. *Gondwana Research*, 23: 701-714. doi:10.1016/j.gr.2012.05.005
- 844 Assumpção, M., Azevedo, P.A., Rocha, M.P., Bianchi, M.B., 2017. Lithospheric Features of the
845 São Francisco Craton. In: M. Heilbron, U. Cordani, F.F. Alkmim (Editors), São Francisco
846 Craton, Eastern Brazil. *Regional Geology Reviews*. Springer, p. 15-25. doi:10.1007/978-3-
847 319-01715-0_2
- 848 Barbarin, B. 1999. A review of the relationships between granitoid types, their origins and their
849 geodynamic environments. *Lithos* 46, 605-626.
- 850 Barbosa, J.S.F., Barbosa, R.G., 2017. The Paleoproterozoic Eastern Bahia Orogenic Domain. In:
851 M. Heilbron et al. (eds.), São Francisco Craton, Eastern Brazil, Regional Geology Reviews.
852 Springer International Publishing: 57-69.
- 853 Beaumont, C., Jamieson, R., Nguyen, M., 2010. Models of large, hot orogens containing a collage
854 of reworked and accreted terranes This article is one of a series of papers published in this
855 Special Issue on the theme Lithoprobe — parameters, processes, and the evolution of a
856 continent. *Canadian Journal of Earth Sciences*, 47: 485-515. doi:10.1139/e10-002
- 857 Beaumont, C., Muñoz, J. A., Hamilton, J., Fullsack, P. 2000. Factors controlling the Alpine
858 evolution of the central Pyrenees inferred from a comparison of observations and
859 geodynamical models. *Journal of Geophysical Research: Solid Earth* 105(B4), 8121-8145.
860 doi/10.1029/1999JB900390
- 861 Belém, J., 2006. Caracterização mineralógica, física e termobarométrica de minérios de grafita da

- 862 Província Gráfica Bahia-Minas, Instituto de Geociências, Universidade Federal de Minas
863 Gerais, 165 pp.
- 864 Butler, J.P., Beaumont, C., Jamieson, R.A. 2013. The Alps 1: A working geodynamic model for
865 burial and exhumation of (ultra)high-pressure rocks in Alpine-type orogens. *Earth and*
866 *Planetary Science Letters* 377-378, 114-131.
- 867 Campos Neto, M.d.C., Basei, M.A.S., Janasi, V.A., Moraes, R., 2011. Orogen migration and
868 tectonic setting of the Andrelândia Nappe system: An Ediacaran western Gondwana
869 collage, south of São Francisco craton. *Journal of South American Earth Sciences*, 32: 393-
870 406. doi:10.1016/j.jsames.2011.02.006
- 871 Caxito, F. A., Uhlein, A., Dantas, E., Stevenson, R., Egydio-Silva, M. & Salgado, S. S. 2017. The
872 Rio Preto and Riacho do Pontal Belts. 221-239.
- 873 Cavalcante, G.C.G., Egydio-Silva, M., Vauchez, A., Camps, P., Oliveira, E., 2013. Strain
874 distribution across a partially molten middle crust: Insights from the AMS mapping of the
875 Carlos Chagas Anatexite, Araçuaí belt (East Brazil). *Journal of Structural Geology*, 55: 79-
876 100. doi:10.1016/j.jsg.2013.08.001
- 877 Cavalcante, C., Hollanda, M. H. B. M., Vauchez, A., Kawata, M. 2018. How long can the middle
878 crust remain partially molten during orogeny? *Geology* 46, 839-842.
- 879 Cavalcante, G.C.G., Vauchez, A., Merlet, C., Berzerra de Holanda, M.H., Boyer, B., 2014.
880 Thermal conditions during deformation of partially molten crust from TitaniQ
881 geothermometry: rheological implications for the anatectic domain of the Araçuaí belt,
882 eastern Brazil. *Solid Earth*, 5: 1223–1242. doi:10.5194/se-5-1223-2014
- 883 Cavalcante, G.C.G., Viegas, G., Archanjo, C.J., da Silva, M.E., 2016. The influence of partial
884 melting and melt migration on the rheology of the continental crust. *Journal of*
885 *Geodynamics*, 101: 186-199. doi:10.1016/j.jog.2016.06.002
- 886 Cavalcante, C., Hollanda, M.H., Vauchez, A., 2018. How long can the middle crust remain
887 partially molten during orogeny? *Geology*, 46 (10), 839-842. doi.org/10.1130/G45126.1
- 888 Chenin, P., Manatschal, G., Picazo, S., Müntener, O., Karner, G., Johnson, C., Ulrich, M. 2017.
889 Influence of the architecture of magma-poor hyperextended rifted margins on orogens
890 produced by the closure of narrow versus wide oceans. *Geosphere* 13(2), 559-576.
- 891 Cruz, S.C.P. and Alkmim, F.F., 2017. The Paramirim Aulacogen. In: M. Heilbron, U. Cordani and
892 F.F. Alkmim (Editors), São Francisco Craton, Eastern Brazil. *Regional Geology Reviews*.
893 Springer, Switzerland, pp. 97-115. doi:10.1007/978-3-319-01715-0_6
- 894 DeCelles, P. G. & DeCelles, P. C. 2001. Rates of shortening, propagation, underthrusting, and
895 flexural wave migration in continental orogenic systems. *Geology* 29, 135-138.
- 896 DeCelles, P. G., Robinson, D. M. & Zandt, G. 2002. Implications of shortening in the Himalayan
897 fold-thrust belt for uplift of the Tibetan Plateau. *Tectonics* 21(6), 12-1-12-25.
- 898 Degler, R., Pedrosa-Soares, A., Dussin, I., Queiroga, G., Schulz, B., 2017. Contrasting provenance
899 and timing of metamorphism from paragneisses of the Araçuaí-Ribeira orogenic system,
900 Brazil: Hints for Western Gondwana assembly. *Gondwana Research*, 51: 30-50. doi:
901 10.1016/j.gr.2017.07.004
- 902 Degler, R., Pedrosa-Soares, A., Novo, T., Tedeschi, M., Silva, L. C., Dussin, I., Lana, C. 2018.
903 Rhyacian-Orosirian isotopic records from the basement of the Araçuaí-Ribeira orogenic
904 system (SE Brazil): Links in the Congo-São Francisco palaeocontinent. *Precambrian*
905 *Research* 317, 179-195.
- 906 Erdős, Z., Huisman, R. S., van der Beek, P., Thieulot, C. 2014. Extensional inheritance and

- 907 surface processes as controlling factors of mountain belt structure. *Journal of Geophysical*
908 *Research: Solid Earth* 119, 9042-9061. doi:10.1002/2014jb011408
- 909 Evans, D.A.D. 2009. The palaeomagnetically viable, long-lived and all-inclusive Rodinia
910 supercontinent reconstruction. *Geological Society Special Publications* 327, 371-404.
911 doi:10.1144/SP327.16
- 912 Evans, D.A.D., Trindade, R.I.F., Catelani, E. L., D'Agrella-Filho, M.S., Heaman, L.M., Oliveira, E.
913 P., Söderlund, U., Ernst, R. E., Smirnov, A.V., Salminen, J. M. 2016. Return to Rodinia?
914 Moderate to high palaeolatitude of the São Francisco/Congo craton at 920 Ma. *Geological*
915 *Society Special Publications* 424, 167-190.. doi:10.1144/SP424.1
- 916 Dias, T. G., Caxito, F. d. A., Pedrosa-Soares, A. C., Stevenson, R., Dussin, I., Silva, L. C. d.,
917 Alkmim, F., Pimentel, M. 2016. Age, provenance and tectonic setting of the high-grade
918 Jequitinhonha Complex, Araçuaí Orogen, eastern Brazil. *Brazilian Journal of Geology* 46,
919 199-219. doi: 10.1590/2317-4889201620160012.
- 920 Dilek, Y., Furnes, H. 2014. Ophiolites and Their Origins. *Elements* 10, 93-100.
- 921 England, P.C., Thompson, A., 1986. Some thermal and tectonic models for crustal melting in
922 continental collision zones. *Geological Society Special Publications* 19, 83–94.
- 923 Faccenda, M., Gerya, T.V., Chakraborty, S., 2008. Styles of post-subduction collisional orogeny:
924 Influence of convergence velocity, crustal rheology and radiogenic heat production. *Lithos*,
925 103(1-2): 257-287. doi:10.1016/j.lithos.2007.09.009
- 926 Faleide, J.I., Tsikalas, F., Breivik, A. J., Mjelde, R., Ritzmann, O., Engen, Ø., Wilson, J., Eldholm,
927 O., 2008. Structure and evolution of the continental margin off Norway and the Barents
928 Sea. *Episodes*, 31: 82-91.
- 929 Fossen, H., Cavalcante, G.C., de Almeida, R.P. 2017. Hot Versus Cold Orogenic Behavior:
930 Comparing the Araçuaí-West Congo and the Caledonian Orogens. *Tectonics* 36, 2159–
931 2178.
- 932 Fuck, R.A., Pimentel, M.M., Alvarenga, C.J.S. and Dantas, E.L., 2017. The Northern Brasília Belt.
933 In: M. Heilbron, U. Cordani and F.F. Alkmim (Editors), *São Francisco Craton, Eastern*
934 *Brazil Regional Geology Reviews*. Springer, pp. 205-220. doi: 10.1007/978-3-319-01715-
935 0_11
- 936 Ganade de Araujo, C.E., Weinberg, R., Cordani, U., 2013. Extruding the Borborema Province
937 (NE-Brazil): a two-stage Neoproterozoic collision process. *Terra Nova*, 26: 157-168.
- 938 Garcia, M.G.M. and Campos Neto, M.d.C., 2003. Contrasting metamorphic conditions in the
939 Neoproterozoic collision-related Nappes south of São Francisco Craton, SE Brazil. *Journal*
940 *of South American Earth Sciences*, 15: 853-870.
- 941 Gonçalves, L., Alkmim, F.F., Pedrosa-Soares, A.C. Dussin, I.A., Valeriano, C.M., Lana, C.,
942 Tedeschi, M. 2016. Granites of the intracontinental termination of a magmatic arc: an
943 example from the Ediacaran Araçuaí orogen, southeastern Brazil. *Gondwana Research*, 36:
944 439-458. doi: 10.1016/j.gr.2015.07.015
- 945 Gonçalves, L., Alkmim, F.F., Pedrosa-Soares, A., Gonçalves, C.C., Vieira, V., 2017. From the
946 plutonic root to the volcanic roof of a continental magmatic arc: a review of the
947 Neoproterozoic Araçuaí orogen, southeastern Brazil. *International Journal of Earth*
948 *Sciences*. doi:10.1007/s00531-017-1494-5
- 949 Gonçalves, L. Farina, F., Lana, C., Pedrosa-Soares, A. C., Alkmim, F. Nalini, H. A., 2014. New
950 U–Pb ages and lithochemical attributes of the Ediacaran Rio Doce magmatic arc, Araçuaí
951 confined orogen, southeastern Brazil. *Journal of South American Earth Sciences*, 52: 129-

952 148. doi: 10.1016/j.jsames.2014.02.008

953 Gradim, C. Roncato, J., Pedrosa-Soares, A. C., Cordani, U., Dussin, I., Alkmim, F. F., Queiroga,

954 G., Jacobsohn, T., Silva, L. C. d. & Babinski, M., 2014. The hot back-arc zone of the

955 Araçuaí orogen, Eastern Brazil: from sedimentation to granite generation. *Brazilian Journal*

956 *of Geology*, 44(1): 155-180. doi:10.5327/z2317-4889201400010012

957 Heilbron, M., Valeriano, C. M., Tassinari, C. C. G., Almeida, J., Tupinamba, M., Siga, O., Trouw,

958 R., 2008. Correlation of Neoproterozoic terranes between the Ribeira Belt, SE Brazil and

959 its African counterpart: comparative tectonic evolution and open questions. *Geological*

960 *Society, London, Special Publications*, 294: 211-237. doi: 10.2113/gselements.7.4.253

961 Horton, F., Hacker, B., Kylander-Clark, A., Holder, R., and Jöns, N., 2016, Focused radiogenic

962 heating of middle crust caused ultrahigh temperatures in southern Madagascar: *Tectonics*,

963 v. 35, p. 293– 314. doi.org/10.1002/2015TC004040.

964 Huismans, R.S., Beaumont, C., 2014. Rifted continental margins: The case for depth-dependent

965 extension. *Earth and Planetary Science Letters*, 407: 148-162.

966 doi:10.1016/j.epsl.2014.09.032

967 Jamieson, R.A., Beaumont, C., 2013. On the origin of orogens. *Geological Society of America*

968 *Bulletin*, 125: 1671-1702. doi:10.1130/B30855.1

969 Jamieson, R.A., Beaumont, C., Fullsack, P., Lee, B., 1998. Barrovian regional metamorphism:

970 Where's the heat? *Geological Society Special Publications*, 138: 23-51.

971 Jamieson, R.A., Unsworth, M.J., Harris, N.B.W., Rosenberg, C.L., Schulmann, K., 2011. Crustal

972 Melting and the Flow of Mountains. *Elements*, 7(4): 253-260.

973 doi:10.2113/gselements.7.4.253

974 Klemperer, S.L., 2006. Crustal flow in Tibet: geophysical evidence for the physical state of

975 Tibetan lithosphere, and inferred patterns of active flow. *Geological Society Special*

976 *Publications*, 268: 39-70.

977 Klootwijk, C.T., Gee, J.S., Pierce, J.W., Smith, G.M., McFadden, P.L., 1992. An early India-Asian

978 contact: paleomagnetic constraints from Ninetyeast ridge, ODP Leg 121. *Geology*, 20: 395–

979 398.

980 Koglin, N., Kostopoulos, D., Reischmann, T. 2009. The Lesvos mafic-ultramafic complex, Greece:

981 Ophiolite or incipient rift? *Lithos* 108, 243-261.

982 Kuchenbecker, M., Pedrosa-Soares, A.C., Babinski, M., Fanning, M., 2015. Detrital zircon age

983 patterns and provenance assessment for pre-glacial to post-glacial successions of the

984 Neoproterozoic Macaúbas Group, Araçuaí orogen, Brazil. *Precambrian Research*, 266: 12-

985 26. doi:10.1016/j.precamres.2015.04.016

986 Li, Y., Wang, C., Dai, J., Xu, G., Hou, Y., Li, X. 2015. Propagation of the deformation and growth

987 of the Tibetan–Himalayan orogen: A review. *Earth-Science Reviews* 143, 36-61.

988 doi:10.1016/j.earscirev.2015.01.001

989 Liou, J. G., Tsujmori, T., Shang, R. Y., Katayama, I., Maruyama, S. 2004. Global UHP

990 metamorphism and continental subduction/collision: the Himalayan model. *International*

991 *Geology Review* 46, 1-27.

992 Long, S., McQuarrie, N., Tobgay, T., Grujic, D. 2011. Geometry and crustal shortening of the

993 Himalayan fold-thrust belt, eastern and central Bhutan. *Geological Society of America*

994 *Bulletin* 123(7-8), 1427-1447. doi:10.1130/b30203.1

995 Magnavita, L., Viana, A.R., Rigoti, C.A., Dehler, N., et al., 2014. The Southeastern Brazilian

996 Margin: Constrains on the Evolution of the São Paulo Plateau. IODP Meeting, Rio de

- 997 Janeiro, Brazil.
- 998 Martins, L., Vlach, S.R.F., Janasi, V.D., 2009. Reaction microtextures of monazite: Correlation
999 between chemical and age domains in the Nazare Paulista migmatite, SE Brazil. *Chemical*
1000 *Geology*, 261: 271-285. doi:10.1016/j.chemgeo.2008.09.020
- 1001 Meira, V.T., García-Casco, A., Juliani, C., Almeida, R.P., Schorscher, J.H.D., 2015. The role of
1002 intracontinental deformation in supercontinent assembly: insights from the Ribeira Belt,
1003 Southeastern Brazil (Neoproterozoic West Gondwana). *Terra Nova*, 27: 206-217.
1004 DOI:10.1111/ter.12149
- 1005 McWilliams, M.O., 1981. Palaeomagnetism and Precambrian tectonic evolution of Gondwana. In:
1006 A. Kröner (Editor), *Precambrian Plate Tectonics*. Elsevier, Amsterdam, p. 649-687.
- 1007 Melo, M.G., Lana, C., Stevens, G., Pedrosa-Soares, A.C., Gerdes, A., Alkmim, L.A., Nalini, H.A.,
1008 Alkmim, F.F., 2017a. Assessing the isotopic evolution of S-type granites of the Carlos
1009 Chagas Batholith, SE Brazil: Clues from U–Pb, Hf isotopes, Ti geothermometry and trace
1010 element composition of zircon. *Lithos*, 284-285: 730-750.
- 1011 Melo, M.G., Stevens, G., Lana, C., Pedrosa-Soares, A.C., Frei, D., Alkmim, F.F., Alkmim, L.A.,
1012 2017b. Two cryptic anatectic events within a syn-collisional granitoid from the Araçuaí
1013 orogen (southeastern Brazil): Evidence from the polymetamorphic Carlos Chagas batholith.
1014 *Lithos*, 277: 51-71.
- 1015 Mondou, M., Egydio-Silva, M., Vauchez, A., Raposo, M.I.B., Bruguier, O., Oliveira, A.F., 2012.
1016 Complex, 3D strain patterns in a synkinematic tonalite batholith from the Araçuaí
1017 Neoproterozoic orogen (Eastern Brazil): evidence from combined magnetic and isotopic
1018 chronology studies. *Journal of Structural Geology*, 39, 158-179.
- 1019 Monié, P., Bosch, D., Bruguier, O., Vauchez, A., Rolland, Y., Nsungani, P., Buta Neto, A., 2012.
1020 The Late Neoproterozoic/Early Palaeozoic evolution of the West Congo Belt of NW
1021 Angola: geochronological (U-Pb and Ar-Ar) and petrostructural constraints. *Terra Nova*,
1022 24(3): 238-247.
- 1023 Moraes, R., Nicollet, C., Barbosa, J. S. F., Fuck, R. A., Sampaio, A. R. 2015. Applications and
1024 limitations of thermobarometry in migmatites and granulites using as an example rocks of
1025 the Araçuaí Orogen in southern Bahia, including a discussion on the tectonic meaning of
1026 the current results. *Brazilian Journal of Geology* 45, 517-539. doi: 10.1590/2317-
1027 4889201520150026.
- 1028 Moura, C.A.V., Pinheiro, B.L.S., Nogueira, A.C.R., Gorayeb, P.S.S., Galarza, M.A., 2008.
1029 Sedimentary provenance and palaeoenvironment of the Baixo Araguaia Supergroup:
1030 constraints on the palaeogeographical evolution of the Araguaia Belt and assembly of West
1031 Gondwana. *Geological Society, London, Special Publications*, 294: 173-196.
1032 doi:10.1144/sp294.10
- 1033 Mouthereau, F., Filleaudeau, P.-Y., Vacherat, A., Pik, R., Lacombe, O., Fellin, M. G., Castelltort,
1034 S., Christophoul, F., Masini, E. 2014. Placing limits to shortening evolution in the
1035 Pyrenees: Role of margin architecture and implications for the Iberia/Europe convergence.
1036 *Tectonics* 33, 2283-2314. doi:10.1002/2014tc003663
- 1037 Munhá, J.M.U., Cordani, U., Tassinari, C.C.G., Paácios, T. 2005. Petrologia e termocronologia de
1038 gnaisses migmatíticos da Faixa de Dobramentos Araçuaí(Espírito Santo, Brasil). 35, 123–
1039 134. *Revista Brasileira de Geociências* 35, 123-134.
- 1040 Noce, C. M., Pedrosa-Soares, A. C., da Silva, L. C., Armstrong, R., Piuzana, D. 2007. Evolution of
1041 polycyclic basement complexes in the Araçuaí Orogen, based on U–Pb SHRIMP data:

- 1042 Implications for Brazil–Africa links in Paleoproterozoic time. *Precambrian Research* 159,
1043 60-78.
- 1044 Oliveira, E.P., Toteu, S. F., Araújo, M. N. C., Carvalho, M. J., Nascimento, R. S., Bueno, J. F.,
1045 McNaughton, N. and Basilici, G., 2006. Geologic correlation between the Neoproterozoic
1046 Sergipano belt (NE Brazil) and the Yaoundé belt (Cameroon, Africa). *Journal of African*
1047 *Earth Sciences*, 44: 470-478. doi:10.1016/j.jafrearsci.2005.11.014
- 1048 Oliveira, E.P., Windley, B.F. and Araújo, M.N.C., 2010. The Neoproterozoic Sergipano orogenic
1049 belt, NE Brazil: A complete plate tectonic cycle in western Gondwana. *Precambrian*
1050 *Research*, 181: 64-84. doi:10.1016/j.precamres.2010.05.014
- 1051 Oriolo, S., Wemmer, K., Oyhantçabal, P., Fossen, H., Schulz, B. & Siegesmund, S. 2018.
1052 Geochronology of shear zones – A review. *Earth-Science Reviews* 185, 665-683.
- 1053 Pedrosa-Soares, A. C., Alkmim, F. F., Tack, L., Noce, C. M., Babinski, M., Silva, L. C. & Martins-
1054 Neto, M. A. 2008. Similarities and differences between the Brazilian and African
1055 counterparts of the Neoproterozoic Araçuaí-West Congo orogen. *Geological Society*,
1056 London, Special Publications 294, 153-172.
- 1057 Pedrosa-Soares, A.C., Campos, C.D., Noce, C.M., Silva, L.C., Novo, T., Roncato, J., Medeiros, S.,
1058 Castaneda, C., Queiroga, G., Dantas, E., Dussin, I.A. and Alkmim, F. F., 2011. Late
1059 Neoproterozoic–Cambrian granitic magmatism in the Araçuaí orogen (Brazil), the Eastern
1060 Brazilian Pegmatite Province and related mineral resources. *Geological Society Special*
1061 *Publications*, 350: 25-51. doi:10.1144/SP350.3
- 1062 Pedrosa-Soares, A.C., Noce, C.M., Wiedemann, C.M. and Pinto, C.P., 2001. The Araçuaí-West-
1063 Congo Orogen in Brazil: an overview of a confined orogen formed during Gondwanaland
1064 assembly. *Precambrian Research*, 110(1-4): 307-323. doi:10.1016/S0301-9268(01)00174-7
- 1065 Pedrosa-Soares, A.C., Vidal, P., Leonardos, O.H. and Brito Neves, B.B., 1998. Neoproterozoic
1066 oceanic remnants in eastern Brazil: further evidence and refutation of an exclusively
1067 ensialic evolution for the Araçuaí-West Congo Orogen. *Geology*, 26: 519–522.
- 1068 Peixoto, E., Pedrosa-Soares, A.C., Alkmim, F.F. and Dussin, I.A., 2015. A suture–related
1069 accretionary wedge formed in the Neoproterozoic Araçuaí orogen (SE Brazil) during
1070 Western Gondwanaland assembly. *Gondwana Research*, 27: 878-896.
- 1071 Petitgirard, S., Vauchez, A., Egydio-Silva, M., Bruguier, O., Camps, P., Monié, P., Babinski, M.
1072 and Mondou, M., 2009. Conflicting structural and geochronological data from the Ibituruna
1073 quartz-syenite (SE Brazil): Effect of protracted “hot” orogeny and slow cooling rate?
1074 *Tectonophysics*, 477: 174-196. doi:10.1016/j.tecto.2009.02.039
- 1075 Pimentel, M.M., 2016. The tectonic evolution of the Neoproterozoic Brasília Belt, central Brazil: a
1076 geochronological and isotopic approach. *Brazilian Journal of Geology*, 46: 67-82.
1077 doi:10.1590/2317-4889201620150004
- 1078 Porada, H., 1989. Pan-African rifting and orogenesis in southern to equatorial Africa and Eastern
1079 Brazil. *Precambrian Research*, 44: 103-136.
- 1080 Reis, H.L.S. and Alkmim, F.F., 2015. Anatomy of a basin-controlled foreland fold-thrust belt
1081 curve: The Três Marias salient, São Francisco basin, Brazil. *Marine and Petroleum*
1082 *Geology*, 66: 711-731. doi:10.1016/j.marpetgeo.2015.07.013
- 1083 Reis, H.L.S. Alkmim, F. F., Fonseca, R.C.S., Nascimento, T.C., Suss, J. F. and Prevatti, L. D.,
1084 2017. The São Francisco Basin. In: M. Heilbron, U. Cordani and F.F. Alkmim (Editors),
1085 São Francisco Craton, Eastern Brazil. Springer, pp. 117-143. doi:10.1007/978-3-319-
1086 01715-0_7

- 1087 Renne, P. R., Onstott, T. C., D'Agrella-Filho, M. S., Pacca, I. G., Teixeira, W. 1990. $^{40}\text{Ar}/^{39}\text{Ar}$
1088 dating of 1.0-1.1 Ga magnetizations from the Francisco and Kalahari cratons: tectonic
1089 implications for Pan-African and Brasiliano mobile belts. *Earth and Planetary Science*
1090 *Letters* 101, 349-366.
- 1091 Reston, T.J., 2010. The opening of the central segment of the South Atlantic: symmetry and the
1092 extension discrepancy. *Petroleum Geoscience*, 16(3): 199-206. Doi:10.1144/1354-079309-
1093 907
- 1094 Rey, P.F., Teyssier, C., Whitney, D.L., 2009. The role of partial melting and extensional strain
1095 rates in the development of metamorphic core complexes. *Tectonophysics*, 477(3-4): 135-
1096 144. doi:10.1016/j.tecto.2009.03.010
- 1097 Rey, P.F., Teyssier, C., Whitney, D.L., 2010. Limit of channel flow in orogenic plateaux.
1098 *Lithosphere*, 2(5): doi:328-332. 10.1130/1114.1
- 1099 Richter, F. Lana, C., Stevens, G., Buick, I.S., Pedrosa-Soares, A.C., Alkmim, F.F., Cutts, K., 2016.
1100 Sedimentation, metamorphism and granite generation in a back-arc region: Records from
1101 the Ediacaran Nova Venécia Complex (Araçuaí Orogen, Southeastern Brazil). *Precambrian*
1102 *Research*, 272: 78-100. doi:10.1016/j.precamres.2015.10.012
- 1103 Robinson, D. M. 2008. Forward modeling the kinematic sequence of the central Himalayan thrust
1104 belt, western Nepal. *Geosphere* 4(5), 785. doi:10.1130/ges00163.1
- 1105 Rosenberg, C. L., Berger, A. 2009. On the causes and modes of exhumation and lateral growth of
1106 the Alps. *Tectonics* 28, doi:10.1029/2008TC002442
- 1107 Sandiford, M., McLaren, S., 2002. Tectonic feedback and the ordering of heat producing elements
1108 within the continental lithosphere. *Earth and Planetary Science Letters*, 204: 133-150.
1109 doi:10.1016/S0012-821X(02)00958-5.
- 1110 Schannor, M., Lana, C. & Fonseca, M. A. 2018. São Francisco–Congo Craton break-up delimited
1111 by U–Pb–Hf isotopes and trace-elements of zircon from metasediments of the Araçuaí Belt.
1112 *Geoscience Frontiers*.
- 1113 Schmid, S. M., Kissling, E. 2000. The arc of the western Alps in the light of geophysical data on
1114 deep crustal structure. *Tectonics* 19, 62-85.
- 1115 Schmitt, R.d.S., Trouw, R., Van Schmus, W.R., Armstrong, R., Stanton, N.S.G., 2016. The
1116 tectonic significance of the Cabo Frio Tectonic Domain in the SE Brazilian margin: a
1117 Paleoproterozoic through Cretaceous saga of a reworked continental margin. *Brazilian*
1118 *Journal of Geology*, 46: 37-66.
- 1119 Schmitt, R.d.S., Trouw, R., Van Schmus, W.R., Pimentel, M., 2004. Late amalgamation in the
1120 central part of Western Gondwana: new geochronological data and the characterization of a
1121 Cambrian collision orogeny in the Ribeira Belt (SE Brazil). *Precambrian Research*, 133:
1122 29-61. doi: 10.1590/2317-4889201620150025
- 1123 Schulmann, K., Lexa, O., Janousek, V., Lardeaux, J. M., Edel, J. B. 2014. Anatomy of a diffuse
1124 cryptic suture zone: An example from the Bohemian Massif, European Variscides. *Geology*
1125 42, 275-278. doi:10.1130/G35290.1
- 1126 Schulmann, K., Lexa, O., P., S., Raeck, M., Tajcmanova, L., Konopásek, J., Edel, J. B., Peschler,
1127 A., Lehmann, J. 2008. Vertical extrusion and horizontal channel flow of orogenic lower
1128 crust: key exhumation mechanisms in large hot orogens? *Journal of Metamorphic Geology*
1129 26, 273-297.
- 1130 Sheth, H. C., Torres-Alvarado, I. S., and Verma, S. P. 2002. What Is the "Calc-alkaline Rock Series"?,

- 1131 International Geology Review, 44:8, 686-701, DOI: 10.2747/0020-6814.44.8.686
- 1132 Stein, S., Engeln, J.F., Wiens, D.A., Speed, R.C., Fujita, K., 1983. Slow subduction of old
1133 lithosphere in the Lesser Antilles. *Tectonophysics*, 99: 139-148.
- 1134 Stern, R. J. 2004. Subduction initiation: spontaneous and induced. *Earth and Planetary Science*
1135 *Letters* 226, 275-292.
- 1136 Szatmari, P., Milani, E.J., 2016. Tectonic control of the oil-rich large igneous-carbonate-salt
1137 province of the South Atlantic rift. *Marine and Petroleum Geology*, 77: 567-596. DOI:
1138 10.1016/j.marpetgeo.2016.06.004
- 1139 Tack, L., Wingate, M.T.D., Liégois, J.-P., Fernandez-Alonso, M., Deblond, A., 2001. Early
1140 Neoproterozoic magmatism (1000–910 Ma) of the Zadinian and Mayumbian Groups (Bas-
1141 Congo): onset of Rodinia rifting at the western edge of the Congo craton. *Precambrian*
1142 *Research*, 110(1-4): 277-306. doi:10.1016/S0301-9268(01)00192-9
- 1143 Tedeschi, M. Novo, T., Pedrosa-Soares, A. C., Dussin, I. A., Tassinari, C. C. G., Silva, L. C.,
1144 Goncalves, L., Alkmim, F. F., Lana, C., Figueiredo, C., Dantas, E., Medeiros, S., Campos,
1145 C. D., Corrales, F., Heilbron, M., 2016. The Ediacaran Rio Doce magmatic arc revisited
1146 (Araçuaí-Ribeira orogenic system, SE Brazil). *Journal of South American Earth Sciences*,
1147 68: 167-186. doi:10.1016/j.jsames.2015.11.011
- 1148 Torsvik, T. H. & Cocks, L. R. M. 2013. Gondwana from top to base in space and time. *Gondwana*
1149 *Research* 24, 999-1030.
- 1150 Trompette, R. 1994. Geology of western Gondwana (2000 - 500 Ma), PanAfrican-Brasiliano
1151 Aggregation of South America and Africa. Balkema Press, Rotterdam, Rotterdam.
- 1152 Trompette, R. 1997. Neoproterozoic (~600 Ma) aggregation of Western Gondwana: a tentative
1153 scenario. *Precambrian Research* 82, 101-112.
- 1154 Trompette, R. 2000. Gondwana evolution; its assembly at around 600Ma. *C. R. Acad. Sci. Paris*,
1155 *Sciences de la Terre et des planètes* 330, 305-315.
- 1156 Turlin, F., Deruy, C., Eglinger, A., Vanderhaeghe, O., André-Mayer, A.-S., Poujol, M., Moukhsil,
1157 A. , Solgadi, F. 2018. A 70 Ma record of suprasolidus conditions in the large, hot, long-
1158 duration Grenville Orogen. *Terra Nova* 30, 233-243. doi:10.1111/ter.12330
- 1159 Uhlein, A., Egydio-Silva, M., Bouchez, J.L., Vauchez, A., 2009. The Rubim Pluton (Minas Gerais,
1160 Brazil): a petrostructural and magnetic fabric study. *Journal of South American Earth*
1161 *Sciences*, 11: 179-189.
- 1162 Valeriano, C.M., 2017. The Southern Brasília Belt. In: M. Heilbron, U. Cordani and F.F. Alkmim
1163 (Editors), *The São Francisco Craton and Its Margins. Regional Geology Reviews*. Springer,
1164 pp. 189-203. doi:10.1007/978-3-319-01715-0_10
- 1165 Valeriano, C.M., Pimentel, M.M., Heilbron, M., Almeida, J.C.H., Trouw, R.A.J., 2008. Tectonic
1166 evolution of the Brasília Belt, Central Brazil, and early assembly of Gondwana. *Geological*
1167 *Society, London, Special Publications*, 294(1): 197-210. doi:10.1144/sp294.11
- 1168 Vauchez, A. Egydio-Silva, M., Babinski, M., Tommasi, A., Uhlein, A., Liu, D., 2007. Deformation
1169 of a pervasively molten middle crust: insights from the Neoproterozoic Ribeira-Araçuaí
1170 orogen (SE Brazil). *Terra Nova*, 19: 278-286. doi:10.1111/j.1365-3121.2007.00747.x
- 1171 Vanderhaeghe, O., 2009. Migmatites, granites and orogeny: Flow modes of partially-molten rocks
1172 and magmas associated with melt/solid segregation in orogenic belts. *Tectonophysics*, 477:
1173 doi:119-134. 10.1016/j.tecto.2009.06.021
- 1174 Vanderhaeghe, O., Burg, J.-P., Teyssier, C., 1999. Exhumation of migmatites in two collapsed

1175 orogens: Canadian Cordillera and French Variscides. In: U. Ring, M.T. Brandon, G.S.
1176 Lister and S.D. Willett (Editors), Exhumation processes: normal faulting, ductile flow and
1177 erosion. Geological Society, London, Special Publications, pp. 181-204.

1178 Vanderhaeghe, O., Duchene, S. 2010. Crustal-scale mass transfer, geotherm and topography at
1179 convergent plate boundaries. *Terra Nova* 22, 315-323.

1180 Vanderhaeghe, O., Teyssier, C., 2001. Partial melting and flow of orogens. *Tectonophysics*, 342:
1181 451-472.

1182 Verniers, J., Pharaoh, T. C., André, L., Denbacker, T. N., de Vos, W., Everaerts, M., Samuelsson,
1183 J., Sintubin, M., Vecoli, M. 2002. The Cambrian to mid Devonian basin development and
1184 deformation history of Eastern Avalonia, east of the Midlands Microcraton: new data and a
1185 review. In: Palaeozoic amalgamation of central Europe (edited by Winchester, J. A.,
1186 Pharaoh, T. C. & Verniers, J.). Geological Society Special Publications 201, 47-93.

1187 Warren, L.V. Quaglio, F., Riccomini, C., Simoes, M. G., Poire, D. G., Strikis, N. M., Anelli, L. E.,
1188 Strikis, P. C., 2014. The puzzle assembled: Ediacaran guide fossil *Cloudina* reveals an old
1189 proto-Gondwana seaway. *Geology*, 42: 391-394. doi:10.1130/g35304.1

1190 Webb, A. A. G., Yin, A., Harrison, T. M., Celerier, J., Gehrels, G. E., Manning, C. E., Grove, M.
1191 2011. Cenozoic tectonic history of the Himachal Himalaya (northwestern India) and its
1192 constraints on the formation mechanism of the Himalayan orogen. *Geosphere* 7(4), 1013-
1193 1061.

1194 Weil, A. B., Yonkee, W. A. 2012. Layer-parallel shortening across the Sevier fold-thrust belt and
1195 Laramide foreland of Wyoming: spatial and temporal evolution of a complex geodynamic
1196 system. *Earth and Planetary Science Letters* 357-358, 405-420.
1197 doi:10.1016/j.epsl.2012.09.021

1198 Winchester, J. A., Pharaoh, T. C., Verniers, J. 2002. Palaeozoic amalgamation of Central Europe:
1199 an introduction and synthesis of new results from recent geological and geophysical
1200 investigations. In: Palaeozoic amalgamation of central Europe (edited by Winchester, J. A.,
1201 Pharaoh, T. C. & Verniers, J.). Geological Society Special Publication 201, 1-18.

1202 Zhang, H. Harris, N., Parrish, R., Kelley, S., Zhang, L., Rogers, N., Argles, T., King, J., 2004.
1203 Causes and consequences of protracted melting of the mid-crust exposed in the North
1204 Himalayan antiform. *Earth and Planetary Science Letters*, 228(1-2): 195-212.
1205 doi:10.1016/j.epsl.2004.09.03
1206